Dissertation Thesis

To earn a Doctoral Degree of Medicine at the Faculty of Medicine of the University of Hamburg

Stimulation of Homologous Recombination by p53 gain-of-function mutant M237I

University Medical Center Hamburg-Eppendorf

Laboratory of Radiation Biology and Experimental Radiation Oncology
Head: Prof. Dr. rer. nat. E. Dikomey
of the Cancer Center Clinics for Radiation Therapy and Radiation Oncology
Head: PD Dr. med. A. Krüll

Presented by Verena Wülfing

Hamburg 2012

Accepted by the Faculty of Medicine

Of the University of Hamburg on: 12th October 2012

Published with the Authority of

The Faculty of Medicine of the University of Hamburg

Examination Board, Chairman: Prof. Dr. J. Dahm-Daphi

Examination Board, 2nd Consultant: PD Dr. K. Borgmann

Examination Board, 3rd Consultant: PD Dr. S. Kindler

1 HYPOTHESIS

Lung cancer is the number one killer of cancer. 85% of lung cancer is non-small cell lung cancer (NSCLC).

About 50% of NSCLC tumors contain p53 mutations. P53 is a protein involved in cell cycle arrest, senescence, apoptosis, differentiation and DNA repair. P53 is the most commonly mutated tumor suppressor gene. A correlation between missing or mutated p53 and the development of cancer is known as well as a correlation between the overexpression of p53-mutants and the bad prognosis of cancer patients.

Homologous recombination is an important repair mechanism for DNA double-strand breaks. In general, homologous recombination is considered as an error-free mechanism. But inappropriate and elevated levels of homologous recombination can lead to genomic instability which may result in cancer development.

P53 is known for its direct interactions with components of the homologous recombination such as Rad51. The tumor suppressor p53 also counteracts hyper-recombination in response to replication fork stalling.

P53 is the most commonly mutated tumor suppressor protein. Most mutations are missense mutations in the DNA-binding core domain of p53. The question to ask is whether the mutant protein inactivates the wild-type function in a dominant-negative fashion or whether the mutants acquire novel functions, a gain-of-function.

Cells containing the p53 mutant M237I showed an increased recombination activity and increased spontaneous and x-ray induced mutation frequencies in comparison to wt p53 cells.

We hypothesize that the p53 mutant M237I is a gain-of-function mutant which may cause a hyper-recombination phenotype eventually promoting carcinogenesis.

2 INTRODUCTIONS

2.1 NON-SMALL CELL LUNG CANCER (NSCLC)

Cancer is a leading cause of death worldwide with lung cancer being the second most common cancer in men and women (see fig. 2.1). It is the leading cause of cancer related deaths in the western world in men and women (Breuer et al., 2005). 30% of cancer deaths in men and 26% in women are caused by lung cancer in the United States (American Cancer Society, 2009). The World Health Organization (WHO) estimates 1.3 million deaths / year are caused by lung cancer (WHO, 2009). 85% of lung cancers are non-small cell lung cancer (NSCLC) (Breuer et al., 2005).

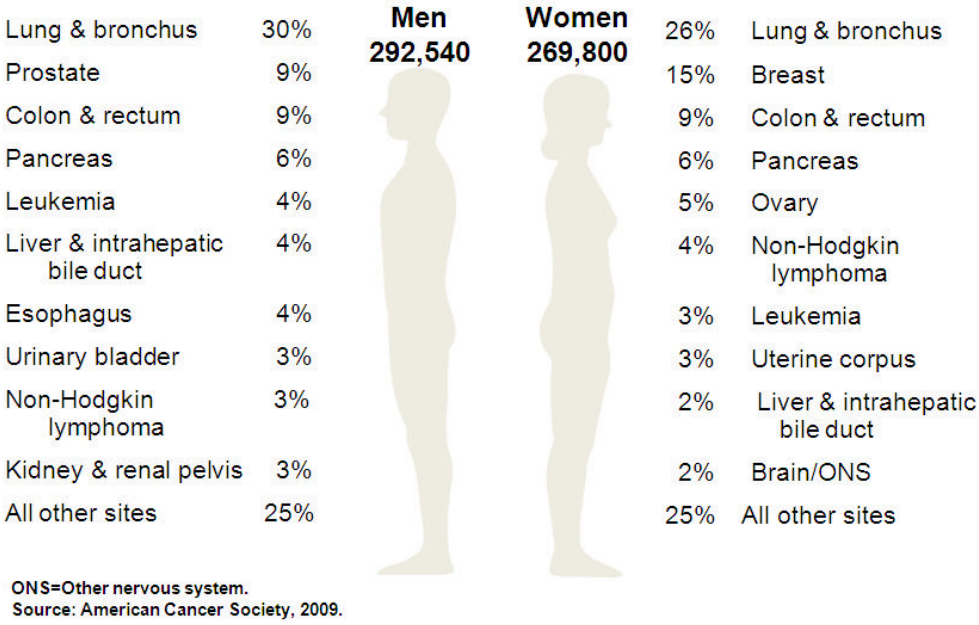

Fig. 2.1: 2009 Estimated US Cancer Deaths (American Cancer Society, 2009). Lung cancer is the leader of cancer deaths in men (30%) and women (26%) in 2009.

Lung cancer is the number one killer of cancer. The prevalence of p53 mutations in non-small-cell lung cancer (NSCLC) is 50%. It is important to study the p53 pathways in these cancer cells to find new targets for an effective therapy that kills the cancer cells but not the normal, non-cancer cells.

2.2 P53

2.2.1 THE TUMOR SUPPRESSOR GENE P53

P53 is a tumor suppressor gene whose activity is highly regulated in mammalian cells. The p53 protein influences the genome integrity through different biochemical and physiological pathways: p53 takes part in the DNA-damage induced G1 arrest

which gives cells time to repair the damage previous to the DNA replication. The protein p53 participates in the regulation of apoptosis which eliminates cells that contain unrepaired DNA damage and it is directly involved in DNA damage repair (Xia and Liber, 1997; Brosh, 2009).
Activated p53 forms a tetramer to function as a transcription factor or repressor. Most of the targeted genes are a part of the regulation of the cell cycle (e.g. p21), apoptosis (e.g. PUMA, Nova, Bax) or DNA-repair-processes (e.g. MSH2 in mismatch repair or p48 in nucleotide-excision repair) (Gatz and Wiesmüller, 2006). This regulation inhibits the propagation of damaged cells. The concentration of the protein p53 is increased if cells get damaged (Bode and Dong, 2004). Overexpression of wildtype (wt) p53 represses the transformation of the cells by the oncogenes MYC and HRAS (Levine and Oren, 2009). An association between impaired p53 function and increasing rates of genetic instabilities (e.g. aneuplodies, allelic losses, increases in sister chromatid exchange, and gene amplification rates) was observed (Gatz and Wiesmüller, 2006).

The p53 gene is known as a tumor suppressor gene and fulfills the following criteria: (i) Tumor cells often do not contain any wt p53 as both alleles are frequently lost by mutations and/or deletions (Levine and Oren, 2009). (ii) P53 mutations were often found to be in at least some cancers a late-occurring event during tumor development. The “loss” plays a part in progression to advanced, invasive and metastatic disease (Levine and Oren, 2009). Intrinsic and environmental factors as well as selection processes produce a selection of p53 mutations in tumors (Brosh and Rotter, 2009). (iii) p53 germline mutations lead to increased cancer susceptibility. (iv) The loss of the p53 gene causes a cancer-prone phenotype in experimental animal models (Levine and Oren, 2009).

The human p53 protein molecular mass is 43.7 kDa (Levine and Oren, 2009). The p53 protein consists of 393 amino acids that include three functional domains. The acidic amino N-terminal domain (amino acids 1-97) acts as transcriptional activation domain that also interacts with Mdm2, the negative regulator of p53. The region of amino acids 98-292 is either called the central, the core, or sequence-specific DNA-binding domain. Most of the interactions between p53 and its target proteins take place by means of the DNA-binding domain (Bode and Dong, 2004). The carboxy C-

terminal end is the tetramerization domain (amino acids 300-393) that contains a nuclear export signal and nuclear localization signals (Bode and Dong, 2004) (see fig. 2.3).

Different types of p53 inactivation are determined in human cancer cells: (i) The protein itself can be mutated or (ii) signaling pathways important for the activation of p53 can be defective (Xu, 2008). The transfection of a p53 mutant into p53-null cells was found to enhance the ability to form tumors in vivo (Shaulsky et al., 1991).
If p53 mutants lose the tumor suppressor functions of wt p53 (Xu, 2008), damaged DNA will not be repaired and those chromosomal instable cells keep on proliferating (Brosh and Rotter, 2009). Chromosomal instability is a hallmark of cancer.
Somatic p53 mutations are found in almost every type of cancer (see fig. 2.2). Rates of somatic p53 mutations differ from 38-50% (Xu, 2008; Schild and Wiese, 2009) in lung, esophageal, colorectal, head and neck, and larynx cancers and to around 5% in sarcoma, testicular cancer, primary leukemia, malignant melanoma, and cervical cancer (Olivier et al., 2010). P53 is the most commonly mutated gene in various human cancers (Xia and Liber, 1997; Xu, 2008; Levine and Oren, 2009; Meek, 2009). There are about 18,000 reports about p53 mutations.

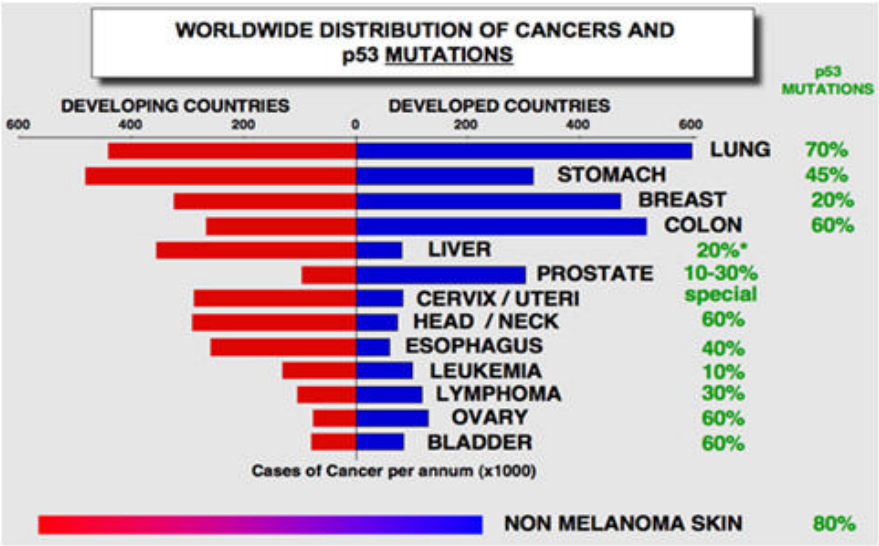

Fig. 2.2: Worldwide distribution of cancers and p53 mutations (http://p53.free.fr; 2009). Lung cancer is a typical example for cancers caused by environmental carcinogens (chemical carcinogens) and smoking which is the reason for higher numbers of lung cancer in developed countries than in developing countries. With 70% lung cancer shows the highest percentage of p53 mutations worldwide, followed by colon, head and neck, ovary and bladder cancer with each 60% p53 mutations.

The most commonly mutated region of p53 is the DNA-binding domain; 86% of the p53 mutations accumulate between the codons 125 and 300 (Hainaut and Hollstein, 2000; Olivier et al., 2010). The majority of these mutations (73%) are missense mutations, leading to a mutant protein that differs to wt p53 by one amino acid caused by a single-nucleotide substitution (Olivier et al., 2009; Olivier et al., 2010). It exists a wide variation of p53 mutants with functional properties differing from mutant to mutant (Bode and Dong, 2004; Olivier et al., 2010).

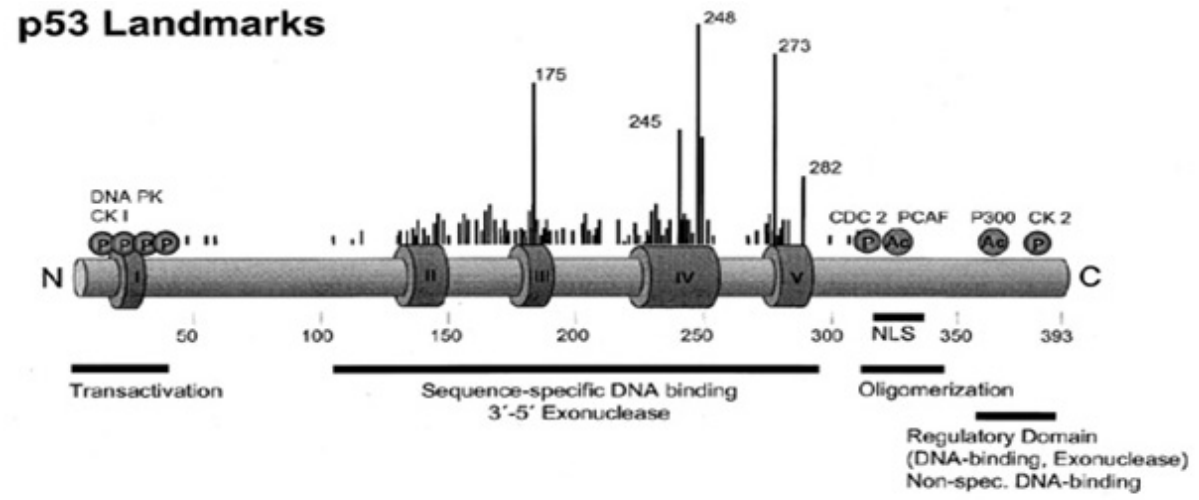

Fig. 2.3: The protein p53 structure and the most commonly mutated regions of p53 (Albrechtsen, 1999). On the left side is the N-terminal transactivation domain. In the middle we see the DNA-binding core domain, the most commonly mutated region of the protein p53 with the hotspot mutants (175, 245, 248 and 273) shown in their incidences. On the right side is the C-terminal regulatory domain.

It was reported about a correlation between the overexpression of p53 mutants and the bad prognosis of cancer patients and an association with poor clinical outcome in a growing array of cancer types (Li et al., 1998; Brosh and Rotter, 2009). Additionally it was found p53 mutations being associated with drug resistance in several malignancies and cell lines (Brosh and Rotter, 2009). Chemotherapy in lung-cancer patients with mutant p53 may decrease the survival of these patients (Ma et al., 2008). The knockdown (stable or conditional) of endogenous mutant p53 reduced the proliferation rate and chemoresistance in vitro; nude mice showed a reduced ability to form tumors (Bossi et al., 2006; Bossi et al., 2008).

2.2.2 P53 MUTANTS IN DETAIL

Wt p53 is an important transcription factor (i) for p21, the key-protein of cell cycle

arrest in G1 phase (Willers et al., 2000), and (ii) for key proteins of apoptosis (Boulon et al., 2010). To exclude the possibility that we see different HR activities in cells with p53 mutants due to cell cycle arrest or apoptosis, the transcription factor activity of p53 had to be impaired.

The p53QS (L22Q/W23S) mutant is an N-terminal (transactivation domain) mutant. Two amino acids are replaced: Leucin is replaced by Glutamin at position 22; Tryptophan is replaced by Serin at position 23 (see fig. 2.4). The p53QS mutant shows an impaired transactivation activity which is 25-30% of the wt p53 activity. The ability to inhibit HR activity is not affected in p53QS cells: p53QS inhibits the HR activity similar to wt p53 (Boehden et al., 2003; Romanova et al., 2004). No inhibition of HR by impaired transactivation activity could be an indication for a direct role of p53 in the HR (Gatz and Wiesmüller, 2006).

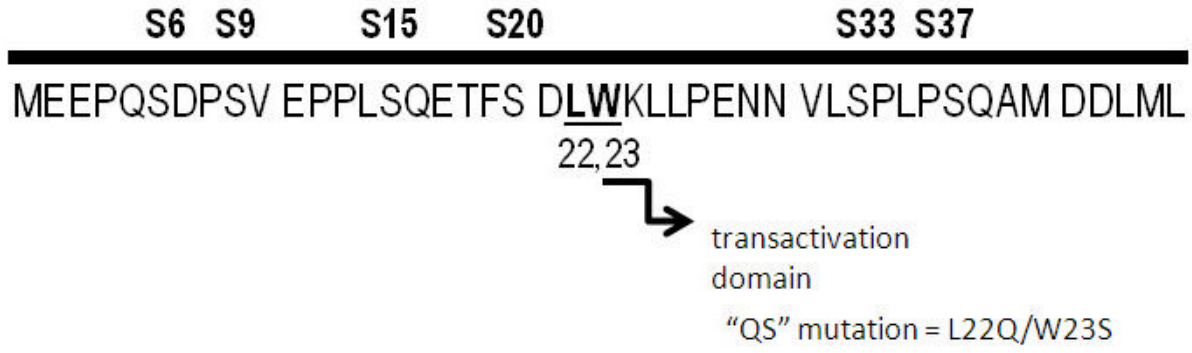

Fig. 2.4: The p53 N-terminal mutant QS (L22Q/W23S). Two amino acids at the N-terminal of p53 are replaced in p53QS (missense mutations): Leucin is replaced by Glutamin at position 22; Tryptophan is replaced by Serin at position 23.

The p53 mutant 273L (Arginin replaced by Leucin at position 273) is one of the hotspot missense p53 mutants. It shows no p53 transactivation activity (Kaneuchi et al., 1999). P53 mutant 273 does not suppress the HR activity (Romanova et al., 2004).

2.3 HOMOLOGOUS RECOMBINATION AND P53

2.3.1 DNA-DOUBLE-STRAND BREAKS (DSBS)

DNA-double-strand-breaks (DSBs), one of the most dangerous DNA lesions, are repaired by homologous recombination (HR) (Rothkamm and Horn, 2009). DSBs can result from different factors, e.g. throughout ionizing radiation (Sengupta and Harris,

2005), chemical agents such as topoisomerase inhibitors, oxidative stress, aberrant V(D)J or class switch recombination (Sedelnikova and Bonner, 2006; Kinner et al., 2008) or indirectly at stalled replication forks / aberrant replication (Helleday et al., 2007). Unrepaired or misrepaired DSBs, and even a single DSB proves detrimental and can cause genomic instability and cancer (Kinner et al., 2008; Srivastava, 2008). Many, maybe all, cancer cells lack one or more aspects of the DNA damage repair because of selective pressures forming the cells during tumor evolution (Jackson and Bartek, 2009). The cancer risk is elevated by error-prone DSB repair, e.g. seen in the large number of breast cancer susceptibility syndromes related to defects in HR surveillance factors (Gatz and Wiesmüller, 2006). As chemotherapy and radiotherapy are based on generating DNA damage in cancer cells, reduced or absent p53 and other pro-apoptotic proteins mostly cause therapy resistance, whereas the treatment of tumor cells with reduced or missing DNA damage repair factors commonly shows a greater therapeutic outcome (Jackson and Bartek, 2009).

2.3.2 HOMOLOGOUS RECOMBINATION (HR)

Chromosomal rearrangements result from incorrect repair of DSBs and seem to be one of the most important initiating factors in carcinogenesis (Reliene et al., 2007; Ismail and Hendzel, 2008; Li and Heyer, 2008). HR uses homologous DNA to repair DSBs (Helleday et al., 2007; Reliene et al., 2007; Cohn and D'Andrea, 2008; Kinner et al., 2008; Li and Heyer, 2008; Hartlerode and Scully, 2009). Therefore, HR represents a key pathway to sustain genomic stability (Li and Heyer, 2008).

HR and non-homologous end-joining (NHEJ) repair DSBs. Cells in S phase mainly repair DSBs through HR (Robison et al., 2007; Branzei and Foiani, 2008; Cohn and D'Andrea, 2008; Srivastava et al., 2008; Jackson and Bartek, 2009); cells deficient in HR show a more reduced repair in S phase than in G1 phase (Hartlerode and Scully, 2009). As chromosomes in G2 and M phase are condensed in a highly ordered chromatin structure, homology search is difficult in those cell phases (Branzei and Foiani, 2008).

HR as DNA-repair-mechanism seems to be an error-free mechanism, in general. Correctly utilized HR supplies a conservative as well as a powerful and necessary DNA DSB repair mechanism (Reliene at al., 2007; Hartlerode and Scully, 2009). Protein Rad51 plays a central role in HR including at stalled replication forks (Janz and Wiesmüller, 2002). The formation of a nucleoprotein filament consisting of

recombinase Rad51 multimers and ssDNA is necessary for the DNA strand invasion and homology search (Helleday et al., 2007; Reliene et al., 2007; Li and Heyer, 2008; Hartlerode and Scully, 2009) in the presence of ATP (Kantake et al., 2003; Li and Heyer, 2008). Through direct protein-interactions wt p53 impairs the Rad51-ssDNA filament formation necessary for continued strand exchange (Gatz and Wiesmüller, 2006; Restle et al., 2008; Schild and Wiese, 2009). The amino acids 125-220 of Rad51 and 94-160 and 264-315 of wt p53 could be identified as taking part in the direct interaction between wt p53 and Rad51 (Sengupta and Harris, 2005; Gatz and Wiesmüller, 2006; Restle et al., 2008; Schild and Wiese, 2009).
HR is a key mechanism for genomic stability and indispensable for life. Homozygous Rad51 null mutation mice died in early embryonic development (Golub et al., 1998; Gatz and Wiesmüller, 2006; Helleday et al., 2007; Reliene et al., 2007) and cells from Rad51-deficient mouse embryos could not be established in cell culture (Sonoda et al., 2007; Reliene et al., 2007).

RPA is known as the eukaryotic ssDNA binding protein (Golub et al., 1998; Kantake et al., 2003; Robison et al., 2007). RPA has functions in replication, repair and recombination of DNA (Robison et al., 2007) as well as in the regulation of transcription (Golub et al., 1998) and checkpoint activation (Branzei and Foiani, 2008). The kinases ATM and ATR are recruited to and activated by DNA DSBs and ssDNA bound by RPA (Jackson and Bartek, 2009). The focal appearance of RPA in S-phase gave evidence of RPA taking part in the replication (Golub et al., 1998). In the HR, RPA initially binds to eukaryotic ssDNA with higher affinity and specificity than Rad51 (Wang and Haber, 2004; Li and Heyer, 2008). RPA is subsequently replaced by Rad51 in a critical and highly regulated process influenced by Chk1 (Kantake et al., 2003; Wang and Haber, 2004; Branzei and Foiani, 2008; Li and Heyer, 2008). RPA facilitates the homologous pairing and DNA strand exchange in the HR (Golub et al., 1998). Accordingly to this close interaction between RPA and Rad51 these two proteins co-localize on synapsed axes in meiosis, in damage induced Rad51 foci or after gamma-irradiation in common foci (Golub et al., 1998). RPA is a heterotrimeric protein (Golub et al., 1998; Robison et al., 2007) that contains of three subunits with 70kDA, 32kDa and 14kDa. Numerous interactions with other proteins are accomplished with the 70kDa subunit (Golub et al., 1998). Residues between the amino acids 168-327 of the 70kDa subunit of RPA are

important for the interaction with human Rad51 (Golub et al., 1998).

Wt p53 binds the 70kDa subunit, preventing RPA from binding to ssDNA in case of spontaneous or DSB-induced HR. The intact binding between wt p53 and RPA is necessary for the suppression of HR by wt p53 (Romanova et al., 2004; Gatz and Wiesmüller, 2006; Reliene et al., 2007). Wt p53's inhibition of RPA binding to ssDNA is independent of the p53 transactivation activity but needs the direct physical interaction with RPA. Mutant p53QS is able to inhibit the RPA binding to ssDNA. P53 mutant 273L co-immunoprecipitates with RPA similar to wt p53 but fails to inhibit HR. The RPA-inhibition is necessary but not sufficient for the HR-inhibition by p53 (Romanova et al., 2004).

2.3.3 HOMOLOGOUS RECOMBINATION AT STALLED REPLICATION FORKS

DSB formation at DNA replication forks was found to be a regular byproduct of the normal DNA replication (Gatz and Wiesmüller, 2006) and there is evidence that DSBs of collapsed replication forks are primarily repaired by HR (Lundin et al., 2002; Sonoda et al., 2007).

Lundin et al. (2002) reported about hydroxyurea causing the collapse of replication forks that result in DSBs which require HR for repair. The collapse and the resulting DSB could be similar to the one caused by a DNA lesion (see fig. 2.5 (a)-(d), modified from Paulsen et al., 2007). Thymidine treatment caused retardation of replication forks without DSBs but also resulting in recombinogenic structures. Lundin et al. (2002) hypothesized a four-way DNA junction, the chicken foot, resulting from DNA reversal/regression, being the recombinogenic structure after thymidine treatment (see fig. 2.5 (e), modified from Postow et al., 2001).

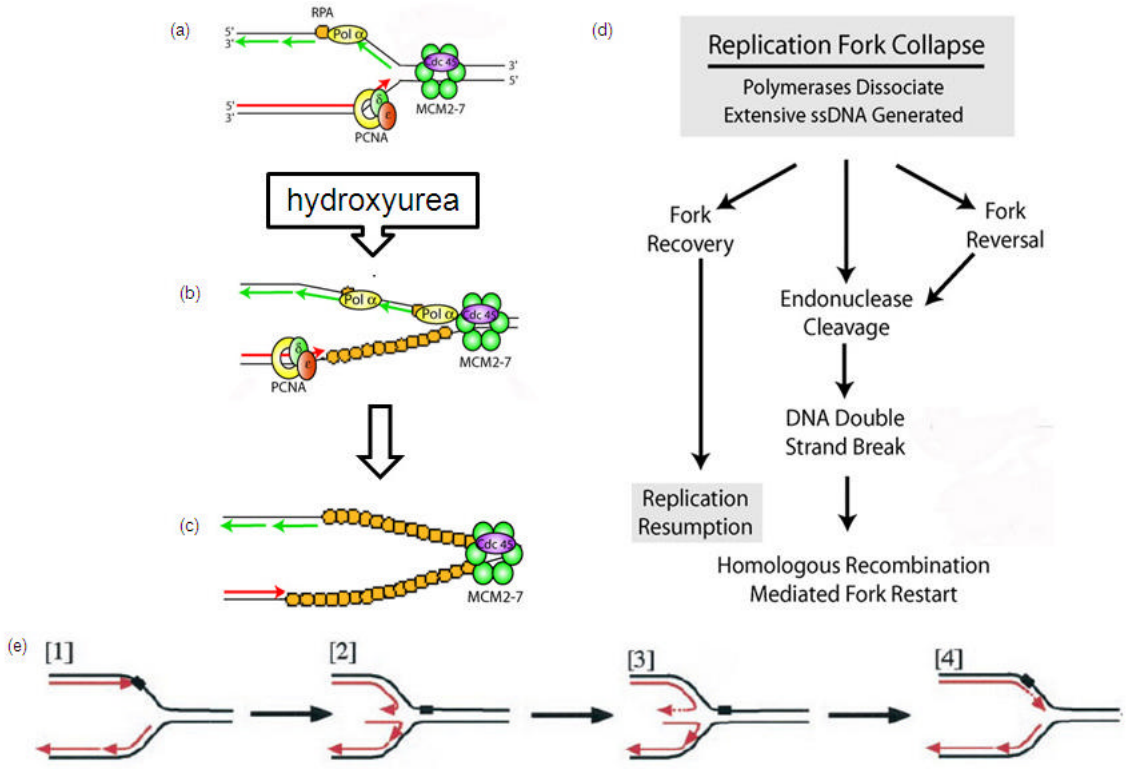

Fig. 2.5: Models of stalled replication forks by replication inhibitors hydroxyurea (a-d) and thymidine (e). (a)-(d) Hydroxyurea model (modified from Paulsen et al., 2007): (a) Intact replication fork. (b) Hydroxyurea blocks the DNA polymerase but not the DNA helicase. An enormous amount of ssDNA is generated. RPA binds to the ssDNA. (c) If the stalled replication fork cannot be stabilized it looses the DNA polymerases and additional ssDNA accumulates; the fork collapses. (d) If DNA polymerases remain unloaded an increasing amount of ssDNA is generated. The ssDNA is removed by endonucleolytic processing by nucleases. This leads to a DNA DSB which can be repaired by HR. DNA replication can be restarted.

(e) Thymidine model (modified from Postow et al., 2001): The stalled replication fork may allow annealing of the nascent leading to the lagging strand, resulting in the formation of a four-way DNA junction, a chicken foot. (3) Without containing a DSB, this four-way DNA junction could be recognized as a substrate for HR at slowed replication forks following thymidine treatment.

2.3.4 HOMOLOGOUS RECOMBINATION IN CARCINOGENESIS

Error-free activity of the HR is dependent on many proteins such as ATM, p53, BRCA, BLM and WRN, Rad51, Rad52, Rad54 and BRCA2. Harmful recombination is mainly caused by the deficiency in HR machinery genes, cell cycle regulators, DNA damage sensory or environmental agents causing DNA damage. This may result in carcinogenesis facilitating genomic rearrangements (e.g. deletions, translocations, duplication, loss of heterozygosity, or aneuploidy). In cancer cells and cancer-prone hereditary human disorders mutations have been found in those genes playing a role in HR (Reliene et al., 2007).

Increased and decreased HR frequencies have been found in cancer cells, with accumulating evidence that impaired HR initiation and resolution plays a role in genetic instability and leads to disease (Helleday et al., 2007; Reliene et al., 2007). Many tumor cell lines and primary tumors show elevated levels (2-7 folds) of Rad51. Rad51 overexpression in tissue culture without any underlying HR repair defect is regularly observed as detrimental to the growth of cells (Schild and Wiese, 2009) and can possibly lead to genomic rearrangements (Reliene et al., 2007) associated with carcinogenesis.

Even though impaired HR activity seems to be a possible step in carcinogenesis, HR suppression was observed to be a late event in tumorigenesis, seen in pancreatic cancer (Helleday et al., 2007).

2.3.5 WT P53 INHIBITS THE HOMOLOGOUS RECOMBINATION (HR)

Wt p53 decreases the activity of the HR (Janz and Wiesmüller, 2002; Romanova et al., 2004; Reliene et al., 2007) on both extra- and intrachromosomal DNA substrates (Sengupta and Harris, 2005; Keimling and Wiesmüller, 2009). The inhibition of the HR by wt p53 is independent of p53's classical role as transcription factor (Akyüz and Boehden, 2002; Janz and Wiesmüller, 2002; Romanova et al., 2004; Sengupta and Harris, 2005; Gatz and Wiesmüller, 2006). Wt p53 is involved in the earliest steps of HR (Gatz and Wiesmüller, 2006). Not only after the production of an artificial DSB but also in response to replication fork stalling does wt p53 prevent hyperrecombination; wt p53 counteracts the accumulation of DSBs at stalled replication forks caused by treatment with UV light or replication elongation inhibitor hydroxyurea (Gatz and Wiesmüller, 2006). Wt p53 inhibits branch migration of the Holiday junction promoted by Rad51, thus, preventing reversal or regression to restart replication (Gatz and Wiesmüller, 2006). An increased level of HR occurs in the absence, inactivation (e.g. by mutation), knockdown or reduced dosage of wt p53 (Bishop et al., 2003; Sengupta and Harris, 2005; Gatz and Wiesmüller, 2006; Keimling and Wiesmüller, 2009). Profound defects in inhibition of HR were seen in experiments for all tested hot spot p53 mutants (Gatz and Wiesmüller, 2006).

Inhibition of HR is mediated by different mechanisms, amongst others through direct interactions with Rad51 and Rad54 (Buchhop et al., 1997; Romanova et al., 2004).

In response to DNA damage wt p53 is phosphorylated by kinases, e.g. through the DNA strand break sensor ataxia teleangiectasia mutated protein (ATM) (Gatz and

Wiesmüller, 2006; Reliene et al., 2007; Restle et al., 2008). Phosphorylated on Serine 15 by ATM and ATR wt p53 represses DSB-induced HR (e.g. when the DNA replication is blocked) through association with key enzymes of the HR such as the MRN complex, Rad51 and RAD54 (Gatz and Wiesmüller, 2006; Restle et al., 2008).

2.4 THE P53 MUTANT M237I – A GAIN-OF-FUNCTION MUTANT

The p53 cancer mutant M237I shows dominant negative properties by comparing two similar human lymphoblastoid cell lines, differing only in the p53 status. The p53 mutation M237I occurs in cancer (Xia et al., 1995).

WTK1 cells (expressing p53 M237I) showed 10 fold increased spontaneously (Xia et al., 1999) and elevated radiation induced gene locus mutations at the autosomal heterozygous thymidine kinase (tk) locus (Xia et al., 1995; Xia et al., 1997) and at the hypoxanthine-guanine phosphoribosyltransferase locus (HPRT) (Chuang et al., 1999). Wt p53 did not affect the mutational process. P53 M237I expressing cells showed a 50 times higher mutation frequency (Chuang et al., 1999) with a higher percentage of large-scale genetic changes than wt p53 cells (Xia et al., 1995).

WTK1 (p53 M237I) cells were less sensitive to radiation induced cytotoxicity than TK6 (wt p53) cells (Xia et al., 1995; Chuang et al., 1999) and showed a delayed apoptotic response to x-rays (Xia et al., 1997). P53 M237I cells were most resistant to the x-ray induced toxicity. WTK1 (p53 M237I) and TK6 (wt p53) cells were compared to p53-null cells. The lack of wt p53 did not lead to increased mutagenesis and only showed slightly more resistance to x-ray induced cytotoxicity. As gain-of-function is defined as a higher HR activity in the mutant cells than in p53-null cells, the increased resistance and elevated mutation frequencies are hypothesized to be due to gain-of-function properties of p53 mutant M237I (Chuang et al., 1999).

P53 M237I mutant expressing cells were observed to catalyze a seven times higher interplasmid recombination activity than wt p53 expressing cells (Xia et al., 1995). The elevated recombinational repair in WTK1 (p53 M237I) cells could contribute to the mutator and hypermutable phenotype (Xia et al., 1995).

2.5 GAMMA-H2AX, A MARKER FOR DNA DOUBLE-STRAND BREAKS

H2AX is one of the most conserved H2A histone variants. Between 2% and 25% of

the H2A pool present in the chromatin is presented by H2AX, varying between cell lines and tissues (Kinner et al., 2008).

As an early event, within minutes after the production of a DNA DSB (Banáth and Olive, 2003; Sonoda et al., 2007) about 2,000 gamma-H2AX molecules (Ismail and Hendzel, 2008) become phosphorylated on serine 139 within the conserved C-terminal region in a 2Mb region around the break. Under normal physiological conditions ATM seems to be the main H2AX phosphorylating kinase (Kinner et al., 2008; Meek, 2009). Phosphorylated H2AX is called gamma-H2AX (Fernandez-Capetillo et al., 2002).

The H2AX phosphorylation facilitates the recruitment of DNA repair proteins (Cohn and D'Andrea, 2008). At low levels of DNA damage the gamma-H2AX mediated recruitment of DNA repair proteins (e.g. 53BP1) seems to be necessary to amplify DNA damage signals. Otherwise damaged cells would enter mitosis without arrest in the cell cycle; damaged cells would proliferate and promote genomic instability (Fernandez-Capetillo et al., 2002; Ismail and Hendzel, 2008). H2AX null cells show deficient recruitment of DNA repair proteins (e.g. 53BP1, BRCA1 and MDC1) in DSB repair foci (Fernandez-Capetillo et al., 2002; Ismail and Hendzel, 2008).

At least in the early stage of repair, the number of gamma-H2AX foci and DSBs seem to be identical and they are a sensitive indicator for DSBs caused by IR or other agents (Rogakou et al., 1998; Banáth and Olive, 2003; Sedelnikova and Bonner, 2006; Bonner et al., 2008; Kinner et al., 2008). Gamma-H2AX molecules form at several more cases than DSB formation, e.g. at single-stranded DNA breaks (Fragkos et al., 2009). We therefore stained cells for 53BPI foci as another marker for DSBs.

2.6 53BPI, A MARKER OF DNA DSBS

The p53 binding protein (53BP1) is one of the downstream signals of gamma-H2AX in response to DNA damage (Fernandez-Capetillo et al., 2002; Sonoda et al., 2005). 53BP1 accumulates quickly at gamma-H2AX foci and is therefore used to detect DNA DSBs (Bonner et al., 2008). Although the 53BP1's initial migration to the DSB is independent of gamma-H2AX (Fernandez-Capetillo et al., 2002; Kinner et al., 2008; FitzGerald et al., 2009) the efficient accumulation and maintenance of the DNA repair proteins such as 53BP1 need the functional presence of gamma-H2AX (Ismail and

Hendzel, 2008; Kinner et al., 2008).

The protein 53BP1 is a central mediator in the DNA damage repair, in the autophosphorylation and activation of ATM, in the ATM-dependent phosphorylation and takes part in the NHEJ (Kobayashi et al., 2008; FitzGerald et al., 2009).

2.7 HYDROXYUREA AND THYMIDINE: REPLICATION ELONGATION INHIBITORS

Thymidine is a replication elongation inhibitor that depletes cells of the deoxyribonucleoside triphosphate dCTP. Cells slow down in their DNA replication activity; the retardation of replication delivers substrates for recombinational repair. In contrast to hydroxyurea, the thymidine treatment following DNA damage is repaired only by HR, and thymidine does not cause DSBs (Lundin et al., 2002). It was hypothesized that the replication complex does not dissociate from the replication fork, the replication fork does not stall and no DNA DSBs result because nucleotides are still incorporated in the DNA after thymidine treatment (Lundin et al., 2002). The retardation of replication delivers substrates for recombinational repair, e.g. the so called chicken foot formation (see fig. 2.5 (e); Postow et al., 2001).

Hydroxyurea is a DNA replication elongation inhibitor that depletes cells of several deoxyribonucleoside triphosphates which leads to replication fork arrest (Lundin et al., 2002; Hartlerode and Scully, 2009). Stalled replication forks lead to DNA DSBs (Lundin et al., 2002; Bonner et al., 2008) that are repaired by HR and non-homologous end-joining (NHEJ). In S-phase hydroxyurea induces HR, visibly by Rad51 foci induction (Lundin et al., 2002).

3 MATERIALS AND METHODS

All materials and chemicals are listed in the supplement.

3.1 CELL LINES

All the experiments were performed in H1299 and A549 cell lines. Both are non-small cell lung cancer (NSCLC) cell lines.

H1299FRT/p53QS, H1299FRTzeo and H1299FRT/p53QM cell lines were derived from the parental H1299 cells (constructed by Willers et al., unpublished). H1299 cells contain a bi-allelic deletion of the p53-gene, therefore do not express the p53 protein.

H1299FRT/p53QS cells contain an N-terminal mutation in the transactivation domain of the p53 protein. Leucin at position 22 is replaced by Glutamin, Tryptophan by Serine at position 23.

H1299FRTzeo cells contain an Flp Recombinase-Target (FRT)-site, a 34bp long sequence that is needed if generating Flp recombinase mediated stable mammalian expression cell lines. The p53 status of H1299FRTzeo cells is p53-null.

H1299FRT/p53QM cells have a p53QS mutation and an additional N-terminal mutation in the RPA-binding domain (W53S/F54S) that abrogates regulation of HR.

A549cDNA and A549/p53-273L are derived from the parental A549 cells. They were constructed by Willers et al. (unpublished). A549 cells express endogenous wt-p53.

A549cDNA cells contain an empty vector (pcDNA3neo) and express wt p53. A549/p53-273L cells a p53 mutated at position 273: Arginin is replaced by Leucin. This changes the DNA binding interface and the expressed p53-mutant is transactivation-deficient and inhibits endogenous wt p53 in a dominant negative manner.

All cells used in the experiments are tested mycoplasma free.

3.2 CELL CULTURE

Cells were cultured in T25 and T75 cell culture flasks. H1299 cells were kept in RPMI 1640 medium, A549 cells in DMEM. All media were enriched with 10% bovine growth serum (BGS), 2% 1x HEPES buffer, 10,000units/ml (1%) Penicillin-Streptomycin and 2mmol/l (1%) L-Glutamine. 200µg/ml Hygromycin B was added as selection antibiotic

to the medium for H1299FRT/p53QS and H1299FRT/p53QM.
Cells were incubated in a humidified 37°C warm incubator with 5% CO_2.

All cell culture work and media preparation were performed in a laminar flow hood in a sterile environment.
Thawing cells out of the liquid nitrogen, a conical vial containing 10^6 cells was placed in the 37°C water bath until partially unfrozen. 1ml of cells from the vial was inserted in a pre-warmed conical tube containing 10ml of medium, followed by gentle mixing. Cells were spun down at 1,000rpm for 2min. Supernatant was poured off and the pellet was resuspended in 4ml of complete-medium, without selection antibiotic. The 4ml were put into a T25 flask in the incubator overnight. The next day the medium was exchanged or cells were passaged depending on the flasks confluency.

Passaging cells, the medium was aspirated and cells were rinsed with 1x PBS (3ml for T25, 5ml for T75). Pre-warmed 1x Trypsin was given to the flask to detach cells (1ml for T25, 2ml for T75). The flask was put in the incubator at 37°C for a few minutes (H1299 for 3min, A549 for 5min). After incubation, the flask was gently shaken by tapping to release any remaining attached cells. The cells were examined under the microscope to ensure a single cell suspension without clumping.
Trypsin was inactivated by adding complete-medium (4ml for T25, 8ml for T75) and the cells were counted with a hematocytometer under the microscope. Cells at a confluency of 70-80% could be used for experiments or dilutions at this point. Otherwise cells were put into flasks at a minimum of 5 x 10^5 cells in a T25 and at a minimum of 10^6 in a T75. Flasks were put into humidified incubator with 5% CO_2 at 37°C.

Cells should normally not be passaged more than 20 - 25 times to keep the experiments uniform. In order to create a stock of cells aliquots of cells were frozen down in a slow freeze process at the earliest possible passage number, 10^6cells/aliquot. Having had trypsinized cells and having had them in a single suspension, they were spun down at 1,000g for 4min. The pellet was resuspended in a 10% Dimethyl Sulfoxide (DMSO) solution in non selective medium which was given time to cool down after preparation. The concentration was 10^6cells/ml. 1ml of this cell suspension was placed into a Cyrogenic vial, kept on ice for 20min and placed in

the -20°C freezer, until frozen (at least 2hours). The vials were transferred into -70°C for the night and transferred into the liquid nitrogen tank not later than 6 months after putting them into -70°C.

3.3 IMMUNOFLUORESCENCE MICROSCOPY

Localization of subnuclear structures by immunofluorescence microscopy makes use of antibodies that are conjugated with fluorescence emitting molecules (fluorochromes) and are specific for the proteins of interest. All experiments were conducted using indirect immunofluorescence microscopy. In this method the fluorochrome Alexa Fluor is coupled to a secondary antibody that is used to recognize the primary antibody-antigen complex. Alexa Fluor 488 was used as conjugate for the secondary antibody. 4',6-diamidino-2-phenylindole (DAPI) was used to visualize nuclei.

The cells were treated with an inhibitor of replication elongation (thymidine or hydroxyurea) at various concentrations and incubation times, fixed and stained. Under a fluorescence microscope the number of foci in 100 nuclei per slide was counted. The number of foci per nucleus was grouped in 0, 1-4, 5-9, 10-14, 15-19 and 20+ foci.

Images were taken of the Alexa Fluor and DAPI staining with the 100x objective and overlayed with the image software Adobe Photoshop 7.0. Contrast and brightness were adjusted if necessary. In the analysis of data, subtracting the control and counting every cell having a certain number of foci (e.g. 5, 10, 15 or 20) as a positive cell, was called "cut-off" (e.g. "5+ cut-off", "10+ cut-off" or "20+ cut-off").

Bars in all graphs represent the means +/- the standard error (s.e.).

3.3.1 RAD51

HR activity can be measured indirectly by monitoring the formation of subnuclear Rad51 foci. For visualizing Rad51 foci, a primary antibody against Rad51 and a secondary Alexa Fluor 488 conjugated antibody were utilized.

$5x10^4$ - $8x10^4$cells/ml were plated in 8 chamber Culture Slides and incubated to let them attach overnight at 37°C. After 18-24h medium was exchanged in the control and cells were treated with thymidine at 1mM or 5mM for 24hours. Medium was

removed and cells were washed with 1x PBS. The fixation of cells was dependent on the cell line. Materials were the same at all times.

H1299 cells were fixed with 100µl/well first. 100µl/well permeabilization buffer were added for 5min, removed and cells were washed with 1x PBS three times. 200µl/well of blocking buffer were added and cells were left at 4°C overnight or 1h at room temperature until staining.
A549 cells became permeabilized with permeabilization buffer at 100µl/well for 5min. Buffer was removed and 100µl/well of fixer were added for 30min. Cells were washed with 1x PBS three times and 200µl/well of blocking buffer were added to each well. Cells were left at 4°C overnight or 1h at room temperature until staining.
The staining began with rinsing the cells once with 1x PBS. Primary antibody Anti-Rad51 Rabbit pAb was added (100µl/well; 1:200 dilution in 2% BSA / 0.1% Triton X/ PBS). Cells were incubated in a humidified chamber at 37°C for 1.5h. The incubation was followed by three washes with 0.1% Triton X / PBS 100µl/well for 5min. The secondary antibody Chicken Anti Rabbit Alexa 488 was added (100µl/well; 1:1000 dilution in 2% BSA / 0.1% Triton X / PBS). Cells were left in a humidified chamber in the dark at room temperature for 1h. Washes (3x5min) with 100µl/well of 0.1% Triton X / PBS and incubation with 100µl/well of DAPI [1µg/ml ddH_2O] at room temperature (2min) followed. Before plastic chamber wells were detached from the chamber slide, cells were washed with 100µl/well of 0.1% Triton X / PBS twice, each 2min. Excess liquid was sucked off and one drop of Antifade per well was added. Cover slips were placed onto slides. Excess Antifade was absorbed by filter paper. Slides and cover slips were sealed with translucent nail polish and slides were stored at 4°C up to two weeks until microscopy.
The foci-counting was conducted under the microscope with the 100x objective. The number of foci in 100 nuclei per slide was counted. The number of foci per nucleus was grouped in 0, 1-4, 5-9, 10-14, 15-19 and 20+ foci.
Images were taken of the Alexa Fluor and DAPI staining with the 100x objective and overlayed with the image software Adobe Photoshop 7.0. Contrast and brightness were adjusted if necessary.

3.3.2 GAMMA-H2AX

Cells were treated with hydroxyurea and thymidine at 1mM and 5mM.
The protocol for gamma-H2AX staining was the same as for Rad51 except for

different treatments and antibodies. The primary antibody was Msm Ab to gamma-H2AX, phospho S139, the secondary antibody was goat anti-mouse IgG (H+L) Alexa Fluor 488.

3.3.3 53BP1

Cells were plated at a density of $5x10^4$ - $8x10^4$ per well. After the attachment (18-24 hours), cells were treated with hydroxyurea at 1mM or thymidine at 5mM for 0h, 2h, 4h, 6h and 24h. After treatment, they were fixed with 3.7% paraformaldehyde in PBS (15min). Cells were washed three times (1x PBS, 5min). Samples were kept at 4℃ until staining. Cells were permeabilized (same permeabilization buffer as for Rad51 staining; 100µl/well; 15 min) and washed with 1x PBS (three times, each 5min). They were incubated in blocking buffer (PBS, 0.1% Triton X, 5% goat serum and 0.2% milk) with 200µl/well at 4℃ overnight. The first antibody Rabbit pAb to 53BP1 (1:200 in PBS, 0.1% Triton X and 3% goat serum) was left on for 45min and cells were washed with 1x PBS four times (each wash 5min). The same secondary antibody as for Rad51 was utilized and left at room temperature for 45min. The culture slides were covered with aluminum foil. Subsequently the cells were washed with 1x PBS four times, each wash 5min. The cells were stained by DAPI [10µg/ml] for 2min. Two washes, each 5min, followed with 1x PBS and the culture slides were detached from the chamber slides. The subsequent procedure was the same as in the Rad51 staining.

3.3.4 RPA

The protocol was the same as for Rad51 and gamma-H2AX except for different treatments and antibodies.

The cells were treated 0h, 2h, 4h, 6h and 24h with thymidine at 5mM. The primary antibody was RPA/p34 Ab-1 (9H8), Mouse MAb, the secondary antibody was goat anti-mouse IgG (H+L) Alexa Fluor 488.

3.3.5 DIFFERENT FIXATIONINGS DO NOT INFLUENCE THE FOCI COUNTING

After 24 hours treatment with thymidine at 5mM, parental A549 cells were fixed in two different ways: Two slides (control and treated cells) were fixed before permeabilization, the other two slides were permeabilized before fixation.

Comparing the results of foci counting in A549 parental cells fixed differently after the

24 hours treatment with thymidine at 5mM, we saw no difference in the percentages of A549 cells being positive for Rad51 signaling in a cut-off of ten and more foci per nucleus . Cells that were fixed before permeabilization were positive for Rad51 signaling in 50%, cells permeabilized before fixation in 51%. In cells fixed before permeabilization as well as in cells permeabilized before fixation, half of the cells were positive. We concluded that different fixationings do not influence the counting of foci.

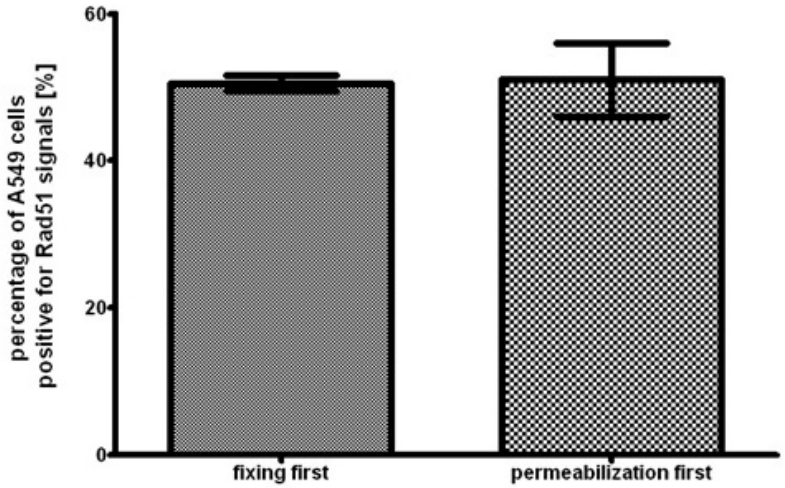

Fig. 3.1: Rad51 foci in A549 cells with different fixationings after 24 hours treatment with thymidine at 5mM showing cells with ten and more foci per nucleus (n = 2). The graph shows the percentages of A549 cells being positive for Rad51 signals (10 or more foci per nucleus) in both cell lines, control subtracted.

3.4 AMPLIFYING PLASMID DNA

The plasmid pcDNAp53Ile237 and the electrocompetent E.coli cells ElectroMAX™ DH10B were thawed on ice. 10µl of bacteria were mixed with 1µl of plasmid DNA [100ng/µl], respectively control pUC19 [10pg/µl]. The 11µl of bacteria and DNA were put in ice chilled electroporation cuvettes (1mm gap). The solution was resuspended and cuvettes were put in the electroporator. The program was set at bacteria ("Ec1"), the time at "ms" and a pulse was given. 1ml of pre-warmed S.O.C. medium was added immediately and content was transferred into a 14ml tube. The tube was put in a shaker at 250rpm at 37°C for 30min. The tube was taken out of the shaker and for each plasmid 5, 25 and 100µl of the solution were stripped on LB-ampicillin-plates [0.1mg/ml]. The plates were put into the incubator for drying at 37°C for 10min without cover on and then turned upside down with cover on overnight (18h).

After incubation the plates were taken out of the incubator. Of the bacterial plates having bacteria colonies expressing pcDNAp53Ile237 on them single colonies were picked with a pipette tip. Two colonies were picked for pcDNAp53Ile237. Pipette tips were put in a 14ml tube with 5ml LB medium with Ampicillin [0.1mg/ml]. Tubes were put in the bacterial shaker (37℃) and shook throughout the day (6-8h). Afterwards 1ml of each of the cloudy 5ml solutions were taken out and put in 250ml LB medium with Ampicillin [0.1mg/ml]. These cultures were shook again with 250rpm at 37℃ overnight (16h). Before the E.coli bacteria were spun down in the centrifuge at 6,000g at 4℃ for 15min, the optical density of the cultures were read with the spectrophotometer. Pellets were frozen down at -20℃.

3.5 PURIFICATION OF PLASMID DNA

The QIAGEN® Plasmid Maxi Kit (Handbook November 2005) was used for the purification of the plasmid DNA pcDNAp53Ile23. It was followed the protocol for high-copy plasmids except for a break after step 12 where the eluate was stored at 4℃ overnight. At step 15, the DNA was redissolved in 200µl TE-Buffer (10mM TrisCl, 1mM EDTA, ph 8.0). The plasmid was frozen down at -20℃ after purification.

PcDNAp53Ile237 was purified out of two different colonies and labeled as “#1” and “#2”. To simplify matters, steps are only described for one of the bacterial solutions but the procedure was the same for the second one as well.

3.6 DNA QUANTIFICATION

DNA concentrations of the purified pcDNAp53Ile237 plasmids were measured with the spectrophotometer GeneQuant pro.

Samples were prepared with 499µl ddH_2O and 1µl DNA. 500µl ddH_2O served as reference. The “DNA” program was used for measurement. The factor was 50, units µg/µl, pathlength 10mm and the dilution factor 500. The reference solution was put into the glass cuvette (10.000mm) first and set as reference. The cuvette was washed three times with ddH_2O afterwards. DNA samples were put into the cuvette and measured. The ratio 260/280 should be around 1.8.

3.7 DNA RESTRICTION DIGEST OF PCDNAP53-M237I#1 AND PCDNAP53-M237I#2

A DNA restriction digest was conducted to confirm the right plasmid was amplified and purified.

In the first step the DNA restriction digest was mixed:

General Protocol	**pcDNAp53237#1**	**pcDNAp53237#2**
2µl 10x Buffer	2µl 10x NE Buffer 3	2µl 10x NE Buffer 3
0.2µl 100x BSA [1mg/ml]	0.2µl 100x BSA	0.2µl 100x BSA
0.5µl restriction enzyme (not more than 10 units/µg DNA)	*PvuI* (10,000 U/ml): 0.5µl	*PvuI* (10,000 U/ml): 0.5µl
0.5µg DNA	0.16 µl [3.0 µg/µl]	0.38µl [1.3 µg/µl]
ddH_2O added up to 20µl	17.14µl ddH_2O	16.92µl ddH_2O

The restriction digest was incubated at 37°C for 1h.

500ml 1x TAE buffer (10ml of 50x TAE buffer plus 490ml ddH_2O) and a 0.8% agarose gel (100ml 1x TAE buffer, 0.8 g agarose and 10µl Ethidium Bromide [5mg/ml]) were prepared.

The 1x TAE and agarose were mixed in a flask and heated in the microwave until the liquid was completely clear. It was poured into the mold and Ethidium Bromide was added. The comb was added and the gel was let set until it was solid (after about 20min). 1x TAE buffer was added until the gel was completely covered, the gel was extracted, turned 90 degrees and set back in again. The comb was extracted.

15µl of DNA ladder were loaded in the first lane. 4µl of loading dye (Orange G loading dye (6X)) were added to each 20µl restriction digest. All 24µl were loaded on the gel from the second lane on.

The uncut controls were prepared as followed:

0.25µl uncut DNA

2.5µl ddH_20

1µl 6x loading dye

The controls were loaded on the gel and the gel ran 2-3h at 80V. The gel was placed under UV light and images were taken. They were printed, scanned and adjusted in contrast and brightness.

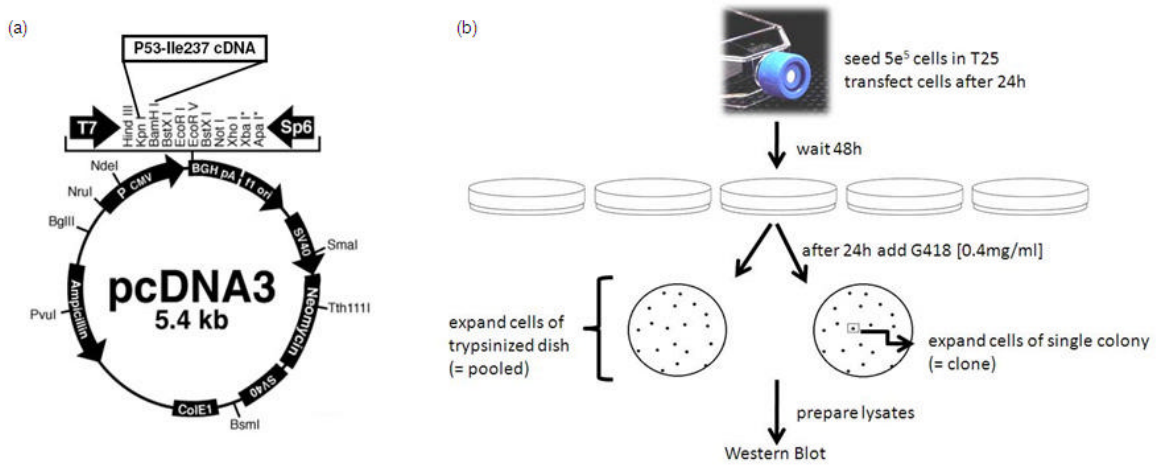

Fig. 3.2: Stable integration of H1299FRT/p53M237I. (a) The p53M237I mutant plasmid pcDNAIle237. The plasmid has a size of 5.4kb and contains two antibiotics resistant genes: ampicillin and neomycin. (b) Stable integration of H1299FRT/p53M237I**.** $5e^5$ cells were seeded in a T25 flask. After 24h cells were transfected and left in the flasks for 48h. Then they were reseeded in petri dishes in different concentrations. After 24h selection antibiotics G418 [0.4mg/ml] was added. Subsequently there were two possibilities to expand cells: all cells of a dish were trypsinized and expanded (on the left side). The cells were pooled. A single cell colony was picked and expanded. All the cells stem from the same clone (on the right side).

Lysates of the single clones and the pooled population were prepared to run a Western Blot. The expression of the protein p53M237I was measured.

3.8 STABLE INTEGRATION OF PCDNAP53-M237I

For creation of the H1299 cell lines which express the mutant p53M237I, H1299FRTzeo cells were transfected with the plasmid pcDNAp53Ile237#2.

Two T25 flasks were prepared with each $5x10^5$ cells in regular medium. They were left in the humidified incubator at 37°C with 5% CO_2 for 18-24h for attachment. The control (pcDNAneo) and the designated plasmid pcDNAp53Ile237, the transfection reagent Metafectene Pro and antibiotic-serum-free-medium were equilibrated to room temperature. The reagents A and B were prepared, combined without mixing and incubated at room temperature for 15min.

Reagent A: 3.3µg of DNA in 100µl serum-antibiotics-free-medium

Reagent B: 20µl of Metafectene Pro in 100µl serum-antibiotics-free-medium

Media were replaced in the flasks with antibiotics-serum-free-medium and the AB-transfection-mix was added. After 3-6h medium was replaced with regular medium and cells were left in the humidified 5% CO_2 incubator at 37°C.
After 48h cells were washed with 1x PBS (3ml), trypsinized (1ml) and dilutions from 10^2 cells/ml to 10^5 cells/ml were prepared. Cells were plated in Petri dishes (100 O.D. x 15 mm H) in different densities: $5x10^2$ and $5x10^3$ cells per Petri dish for cDNAneo3, $5x10^2$, 10^3, $5x10^3$, 10^4 and 10^5 cells per Petri dish for pcDNAp53Ile237#2. Petri dishes were put in the humidified incubator with 5% CO_2 at 37°C.
Medium was replaced after 18h with medium that contained the selection antibiotic G418 [400 mg/ml]. Media was exchanged from this point on every five days.
After 2-3 weeks colonies could be seen and two possibilities were taken to continue depending on which kind of cells were designated.

A) Single clones
In this population, all cells derived from the same cell and formed a colony. Cells were all identical. To receive a single clone a single colony was picked.
Designated colonies were detached with a drop of 1x Trypsin. Cells were picked with a pipette tip and put in a well of a 24-well-plate. Cells were kept in medium with selection antibiotic G418 which was exchanged every five days. Cells were left in the wells up to 100% confluency (around 21 days) before being transferred to T25 flasks. Cells were kept in cell culture as described above (3.2).

B) Pooled population
A pooled population was a population that derived from different cells. Not all cells were identical. To obtain a pooled population a whole Petri dish was trypsinized.
The procedure was the same as described for single clones except for the first step: Not a single clone was picked but the whole dish was trypsinized and put in a well of a 24-well-plate.

3.9 TRANSIENT TRANSFECTION OF PCDNAP53-M237I

The transient transfection was the same as the stable transfection to the step of selection with the antibiotic G418 for cDNAp53Ile237 expressing colonies.
Directly after colonies had grown in Petri dishes, cells were used for immunofluorescence microscopy experiments.

3.10 TOTAL CELL LYSATES

Petri dishes (10^6cells/dish) were plated one day before the preparation of lysates. When cells had attached after 18h the lysis buffer was mixed:

0.5 ml Biosource Buffer
2.5 µl phenylmethylsulfonyl fluoride (PMSF)
5µl Protease Inhibitor Cocktail

Lysis buffer, 1x PBS, Petri dishes and microcentrifuge tubes were put on ice. Medium was removed from the first Petri dish. Cells were rinsed with ice cold 1x PBS twice. 20µl of lysis buffer was added and incubated on ice for 90min. Cells were scraped from the dish and the collected lysate was put in an ice-cold 1.5ml tube. These steps were repeated for all Petri dishes. Subsequently lysates were incubated on ice for 30-45min and spun down at 12,000rpm at 4℃ for 12min. The supernatant was collected in ice-cold 1.5ml tubes. Samples for the protein concentration assay were prepared before the aliquotted lysates were frozen at -20℃.

3.11 PROTEIN CONCENTRATION ASSAY

It was necessary to measure the concentrations of the lysates to load a certain amount of protein on the western blot gel. The concentrations were measured with the spectrophotometer GeneQuant pro at a wavelength of 595nm. A standard curve with diluted BSA was set as reference for calibration purposes.
The samples of lysates were prepared as followed:

Tube	**Lysate (µL)**	**ddH2O (µL)**	**Dye Concentrate (µL)**
Reference	0	800	200
Sample	2	798	200

3.12 WESTERN BLOT

3.12.1 RUNNING THE WESTERN BLOT GEL

Samples were set up as followed:

6.3µl of protein and ddH_2O
6.25µl 4x Sample Buffer
2.5µl of 10x Reducing Agent

To load the same amount of protein of each sample, the amount of protein in 16.3µl of the sample with the lowest protein concentration was calculated. The same amount of protein was loaded for the other samples with ddH_2O added to the protein. In total, 16.3µl of protein and ddH_2O were mixed with Sample Buffer and Reducing Agent in each sample.

The tubes containing the whole 25µl of the sample were pulse-spun. The protein was denatured by heating it up at 70°C in the heat block for 10min. While heating up the samples, a 4-12% Bis-Tris Gel and 1x MES SDS Running Buffer were prepared and the protein standard was thawed. The running apparatus was assembled: Around 200ml of MES SDS Running buffer were filled in the inner chamber. The outer chamber was filled with around 600ml of the MES SDS Running Buffer.

The heated samples were cooled down on ice for 1min and pulse-spun. 17µl of protein standard were loaded in the first lane, 25µl of each sample in the remaining lanes. The gel ran 1h at 150V and 1h at 175V with 0.08A.

3.12.2 TRANSFERRING THE WESTERN BLOT GEL

10% methanol makes the bands sharper for small proteins under 50kDa. It was given to the Transfer Buffer which was prepared as followed and chilled at 4°C:

50ml Transfer Buffer (20x)
10ml 10% SDS Sodium Dodecyl Sulfate Solution
100ml Methanol
840ml ddH_2O

The membrane was washed briefly in methanol, ddH_2O and chilled transfer buffer. The membrane was kept wet from this point on at all times. The membrane was chilled at 4°C.

The gel, two pieces of filter paper and two sponges were soaked in chilled transfer

buffer. The transfer cassette was also put in transfer buffer and the sandwich was assembled in the following order without air bubbles: One sponge was put on the positive side of the cassette, followed by a filter paper, the membrane, the gel and finally another filter paper and the second sponge. Each layer was soaked well in buffer at all times.

Half of the transfer apparatus was filled up with transfer buffer, the cooling block was put in and the remaining buffer was added. The gel ran at 100V and 0.26A for 1h. The blotted membrane was put in 10ml blocking buffer (5% dried milk in 0.1% T-TBS) at 4℃ overnight (14h).

3.12.3 BLOTTING FOR P53

The membrane was cut through and rinsed briefly with 0.1% T-TBS. Each half was incubated with its primary antibody: The upper half with Filamin-1 (E-3) mouse monoclonal IgG_2a sc-17749 (1:1,000 in blocking buffer), the lower half with Anti-p53 (Ab-7) (Pantropic) Sheep pAb (1:1,000 in blocking buffer). Antibodies were left on for 150min. The membrane was washed on a shaker three times in at least 150ml of 0.1% TBS-T at room temperature for 10 minutes and incubated with the secondary antibody (1h on the shaker at room temperature). The upper half was incubated with goat anti-mouse IgG-HRP sc-2031 (1:10,000 in blocking buffer), the lower one with donkey anti-sheep IgG-HRG sc-2473 (1:10,000 in blocking buffer).

Subsequently the membrane was washed on a shaker three times in at least 150ml of TBS-T at room temperature for 10min.

3.12.4 VISUALIZING THE BLOTTED PROTEINS

The membrane was placed (face up) inside a transparency and a 1:1 solution of ECL detection reagents was spread on the membranes. The excess ECL reagent was removed. The membrane was not dried completely and no pockets with excess ECL between the membrane and transparency were left over. The transparency including the membrane was taped into a film cassette and the membrane was exposed to film in the dark room for the desired times (1, 2 and 5min). The film was developed in the dark room. The images were digitalized with a scanner and adjusted with Adobe Photoshop 7.0 in contrast and brightness.

3.13 ANALYSIS OF RELATIVE EXPRESSION LEVELS OF PROTEINS

The scanned image of the membrane was opened with the software ImageJ. The image was inverted ("Invert"). Every band was marked with the same "Rectangular selection", the integrated density ("IntDen") of the band was memorized by pressing "Strg + M". This step was repeated for every filamin and p53 band. The file with the memorized integrated densities was saved and opened with the spreadsheet application software Microsoft Office Excel 2007. The ratio of "IntDen" of p53 divided by "IntDen" of filamin was calculated for every sample. The ratios of the different samples were relatively compared to each other.

3.14 PRELIMINARY TEST RESULTS

3.14.1 OD600 READING

In order to create the p53-mutant M237I, E.coli ElectroMAX™ DH10B™cells were transformed with the plasmid pcDNAp53M237I for amplification. The optical density of two single transformed colonies was measured in order to measure the cell density. It is important to use the right number of cells to get optimal results in the plasmid purification.

The optical density (OD) of the two E.coli-solutions was measured with the spectrophotometer. To receive optimal results in the plasmid purification, the cell density should be approximately 3 - 4*10^9 cells/ml which refers to a pellet wet weight of approximately 3g/liter medium.

For pcDNAp53M237I#1 the OD was 1.836g/ml.
For pcDNAp53M237I#2 the OD was 1.784g/ml.

The OD is multiplied by the total bacteria volume (250ml). The result is the total bacteria mass.

pcDNAp53M237I#1: 1.836g/ml*250ml = 459g
pcDNAp53M237I#2: 1.784g/ml*250ml = 446g

3.14.2 DNA CONCENTRATION ASSAY

After the plasmid purification of pcDNAp53M237I#1 and pcDNAp53M237I#2 we

measured the concentrations of the plasmids. Knowing the concentrations, we could subsequently load the DNA samples for a DNA restriction digest to verify we amplified the right plasmid. For the following transient and stable transfection it was also necessary to know the plasmid's concentrations.

The DNA concentration was measured with the spectrophotometer GeneQuant pro after plasmid purification. All three plasmids showed a concentration about 1 µg/µl.

DNA sample	**Concentration [µg/µl]**
cDNAneo	1.1
pcDNAp53M237I#1	0.9
pcDNAp53M237I#2	1

3.14.3 DNA RESTRICTION DIGEST OF PCDNAP53-M237I#1 AND PCDNAP53-M237I#2

In a DNA restriction digest the purifications of pcDNAp53-M237I#1 and #2 were verified. The cut and uncut version of each plasmid were loaded on the gel. Uncut plasmids ran at 3.0kb, the cut versions at about 5.4kb.

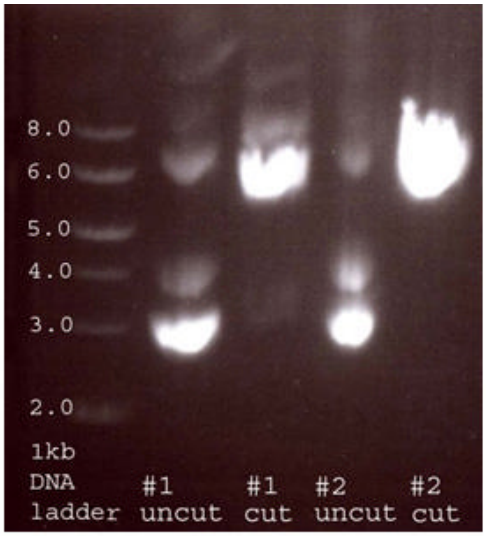

Fig. 3.3: DNA restriction digest of pcDNAp53M237I#1 and pcDNAp53M237I#2. The first lane (left) shows the 1kb DNA ladder, lane 2 and 3 show the uncut and cut plasmid pcDNAp53M237I#1, lane 4 and 5 the uncut and cut plasmid pcDNAp53M237I#2.

3.14.4 PROTEIN CONCENTRATION ASSAY OF P53M237I-MUTANTS FOLLOWING STABLE TRANSFECTION

Stable transfection of cells ensures that the transfected gene is integrated into the

genome of the cell. Daughter cells will inherit the gene information and will also express the transfected gene.

Additionally to the p53-mutant M237I encoding gene we did transfect the cells with an antibiotics resistant gene against G418. Adding G418 to the medium we selected for transfected cells that stably kept the mutant p53 M237I gene presumably due to integration. For verification that cells further expressed the p53 mutant M237I protein we prepared lysates for a western blot.

Lysates of p53M237I-mutant cells assembled with stable transfection and H1299FRTzeo were prepared and the protein concentrations were measured with the spectrophotometer.

The concentration varied between 1.75µg/µl in H1299FRT/p53M237I C7 and C9 and 2.95µg/µl in H1299FRT/p53M237I pooled cells. H1299FRT/p53M237I C4 and H1299FRTzeo show a concentration of 1.95µg/µl. H1299FRT/p53M237I C8 has a lower one of 1.9µg/µl. The H1299FRT/p53M237I clones C5, C6 and C12 were measured with protein concentrations around 2µg/µl (2.2µg/µl, 2.1µg/µl and 2.0µg/µl).

Sample	**Protein Concentration [µg/µl]**
H1299FRT/p53M237I C4	1.95
H1299FRT/p53M237I C5	2.2
H1299FRT/p53M237I C6	2.1
H1299FRT/p53M237I C7	1.75
H1299FRT/p53M237I C8	1.9
H1299FRT/p53M237I C9	1.75
H1299FRT/p53M237I C12	2.0
H1299FRT/p53M237I pooled	2.95
H1299FRTzeo	1.95

4 RESULTS

4.1 WT P53 SUPPRESSES THE HOMOLOGOUS RECOMBINATION ACTIVITY

To establish the impact of wt p53 on HR, we utilized an isogenic pair of A549 cells differing only in the p53 status: A549cDNA cells are cDNA vector-alone transfected A549 cells expressing wt p53. A549/p53-273L cells express the dominant-negative p53 mutant 273L having no p53-specific transactivation activity (Kaneuchi et al., 1999).

The HR activity in A549 cells was measured by the ability of cells to form subnuclear Rad51 foci in response to replication stalling. There might be two subsequent replication restart mechanisms to stalled replication forks: one with and the other one without forming a DSB. Rad51 possibly mediates both mechanisms. There is evidence that Rad51 foci form only in the HR process at collapsed replication forks and not at the restart of stalled replication forks (Petermann et al., 2010). Replication forks collapse by generation of DSBs (Petermann and Helleday, 2010). An increasing number of DSBs is generated after more than 12 hours of replication fork stalling (Saintigny et al., 2001). In our experiments we treated cells for 24 hours with thymidine at 5mM, so probably the majority of replication forks collapsed. In the following Rad51 can be taken as a surrogate for collapsed forks that are repaired by HR.

To compare untreated cDNA vector-alone transfected A549cDNA cells expressing endogenous wt p53 with untreated A549/p53-273L cells which express the dominant-negative p53 mutant 273L, the majority (43% of A549cDNA and 35% of A549/p53-273L) of untreated cells in both cell lines showed no Rad51 foci per nucleus (shown in fig. 4.1 (a) – (d)). In untreated cells 41% of A549cDNA cells and 42% of A549/p53-273L cells had 1-4 Rad51 foci per nucleus. In both cell lines less than five percent of untreated cells had ten or more Rad51 foci per nucleus.
After the treatment with thymidine (5mM, 24 hours), an inhibitor of replication elongation, about half of the treated A549cDNA (44%) and A549/p53-273L cells (52%) showed ten or more Rad51 foci per nucleus.

Comparing cells with ten and more foci per nucleus (shown in fig. 4.1 (e)) showed a difference in the percentage of cells being positive for Rad51 signaling between

A549cDNA (wt p53) and A549/p53-273L (dominant-negative mutant) cells of 8%: p53-273L cells (52%) had more Rad51 foci per nucleus than wt p53 cells (44%). Differences in Rad51 foci are due to a different number of collapsed replication forks in the cells that are repaired by HR. As the dominant-negative mutant p53-273L expressing cells showed more Rad51 foci than wt p53 expressing cells we interpreted the results as a suppression of HR by wt p53 as published by numerous groups before (Janz and Wiesmüller, 2002; Romanova et al., 2004; Sengupta et al., 2005; Reliene et al., 2007; Restle et al., 2008).

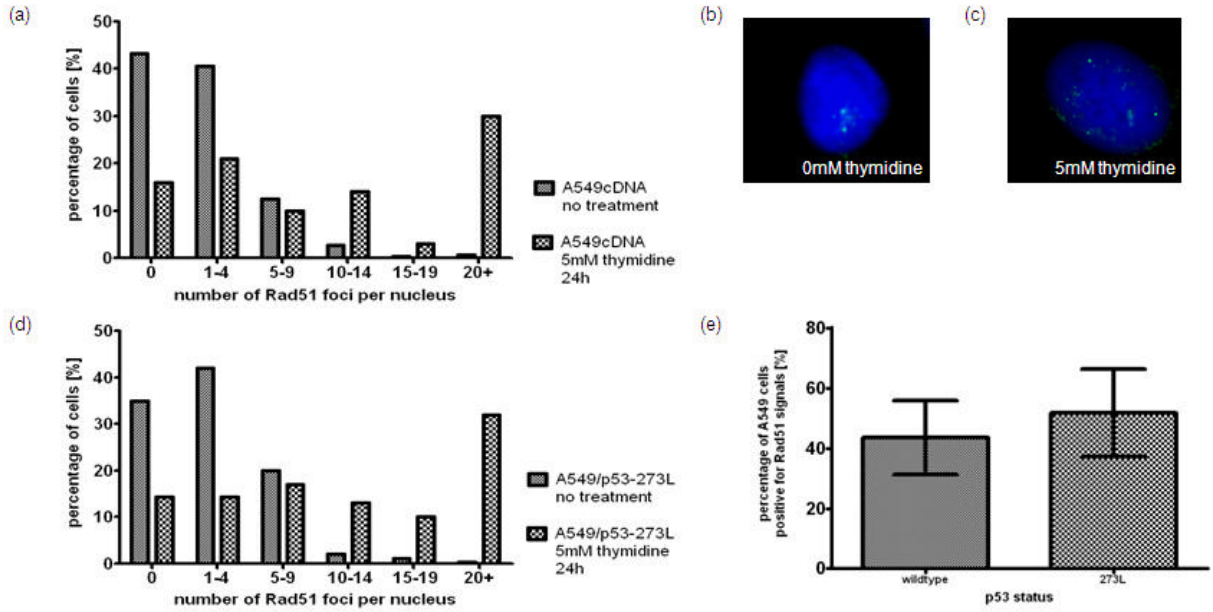

Fig. 4.1: Rad51 foci in A549cDNA and A549/p53-273L cells after 24 hours treatment with thymidine at 5mM (n = 3). (a) Percentage of untreated A549cDNA cells that exhibit nuclear Rad51 foci and after the treatment with thymidine (5mM, 24h). (b) Photograph of an A549cDNA control cell with two Rad51 foci. (c) A549cDNA cell after the treatment with thymidine (5mM, 24h) with five Rad51 foci. (d) Percentage of untreated A549/p53-273L cells that exhibit nuclear Rad51 foci and after the treatment with thymidine (5mM, 24h). (e) Rad51 foci in A549cDNA and A549/p53-273L after 24 hours treatment with thymidine at 5mM showing cells with ten and more foci per nucleus (n = 3). The graph shows the percentages of cells being positive for Rad51 signals (10 or more foci per nucleus) in both A549 cell lines, control subtracted.

4.2 P53QS SUPPRESSES THE HR ACTIVITY IN COMPARISON TO P53-NULL CELLS

We saw a suppression of HR by wt p53. To demonstrate, that this suppression is independent of the transcription factor activity of p53 (Janz and Wiesmüller, 2002;

Romanova et al., 2004), we conducted the same experiment as in A549 cells (shown in fig. 4.1) in H1299 cell lines. As H1299 cells do not express wt p53, we used the cell line H1299FRTzeo that were p53-null, cDNA vector-alone transfected cells, and H1299FRT/p53QS cells that express the p53 N-terminal mutant L22Q/W23S. The QS mutation is located in the transactivation domain and inhibits the binding of p53 to the DNA. Therefore H1299FRT/p53QS cells show a transcription factor activity that is only 25-30% of the one of wt p53 (Romanova et al., 2004).
Expressing the p53 mutant impaired in its transcription factor activity, 78% of untreated H1299FRT/p53QS cells showed nine or less Rad51 foci per nucleus, compared to 70% in untreated H1299FRTzeo cells (shown in fig. 4.2 (a) – (d)).
After the treatment with thymidine (5mM, 24h) the majority of 97% in H1299FRTzeo cells had ten or more foci per nucleus, whereas 58.55% of treated H1299FRT/p53QS cells showed ten or more foci per nucleus.

Comparing H1299FRT/p53QS and H1299FRTzeo cells with 20 and more foci per nucleus after the treatment with thymidine (5mM, 24h) shown in fig. 4.2 (e) showed a difference in the percentage of cells being positive for Rad51 signaling between the cell lines of 51%. P53-null cells (77%) had more Rad51 foci per nucleus than p53QS expressing cells (26%).

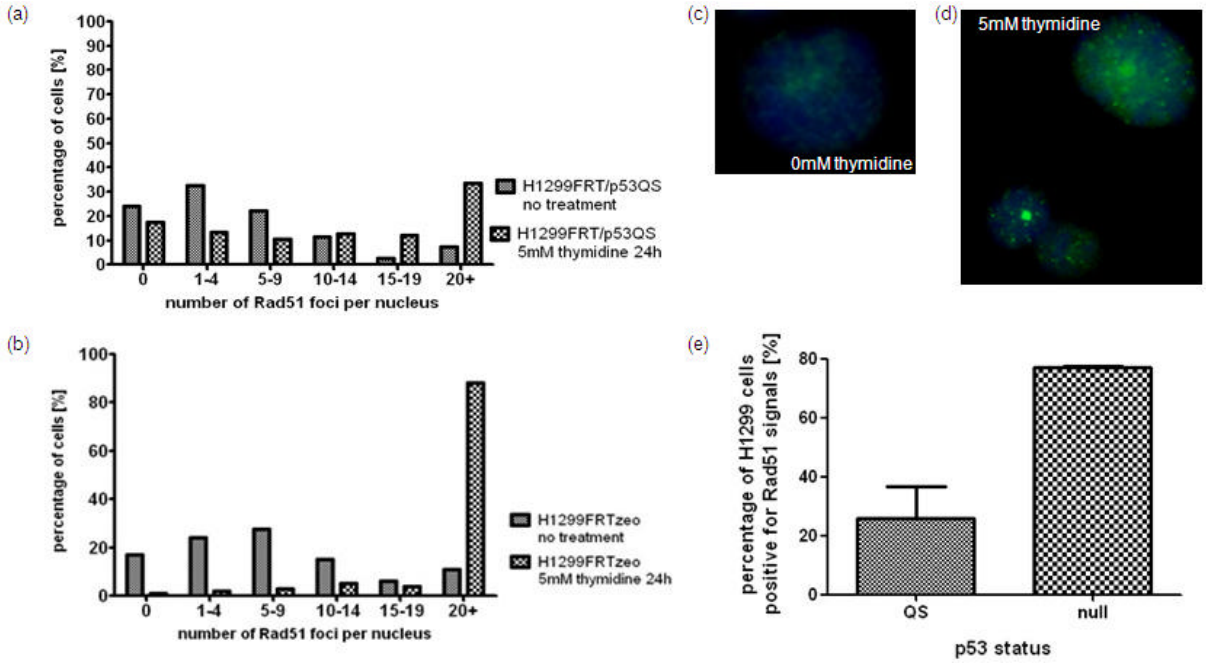

Fig. 4.2: Rad51 foci in H1299FRT/p53QS and H1299FRTzeo cells after 24 hours treatment with thymidine at 5mM (n = 2). (a) Percentage of untreated H1299FRT/p53QS cells that exhibit nuclear Rad51 foci and after the treatment with thymidine (5mM, 24h). (b) Percentage of untreated H1299FRTzeo cells that exhibit nuclear Rad51 foci and after the treatment with thymidine (5mM, 24h). (c) Photograph of an H1299FRTzeo control cell without Rad51 foci. (d) Photograph of three H1299FRTzeo cells after the treatment with thymidine (5mM, 24h) with each more than 10 Rad51 foci. (e) Rad51 foci in H1299FRT/p53QS and H1299FRTzeo cells after 24 hours treatment with thymidine at 5mM showing cells with twenty and more foci per nucleus (n = 2). The graph shows the percentages of H1299 cells being positive for Rad51 signals (20 or more foci per nucleus) in both cell lines, control subtracted.

The treatment of H1299FRTzeo and H1299FRT/p53QS cells with thymidine (5mM, 24h) produced high percentages of cells being positive for Rad51 signaling, having twenty or more Rad51 foci per nucleus. To ensure we could see the eventual gain-of-function of the p53 M237I mutant showing a higher percentage of positive cells than H1299FRTzeo cells we repeated the experiment shown in fig. 4.2 with a five times lower concentration of thymidine at 1mM.

Shown in fig. 4.3 (a)-(d), 5% of untreated H1299FRT/p53QS and 10.5% of H1299FRTzeo cells showed ten or more Rad51 foci per nucleus. After the treatment with thymidine (1mM, 24h), 47.85% of H1299FRTzeo and 14.3% of H1299FRT/p53QS cells showed ten or more Rad51 foci per nucleus.

In summary, after the treatment with thymidine (1mM, 24h) there were four times as much H1299FRTzeo cells (36%) positive for Rad51 foci compared to

H1299FRT/p53QS cells (9%) with ten and more foci per nucleus (shown in fig. 4.3 (e)).

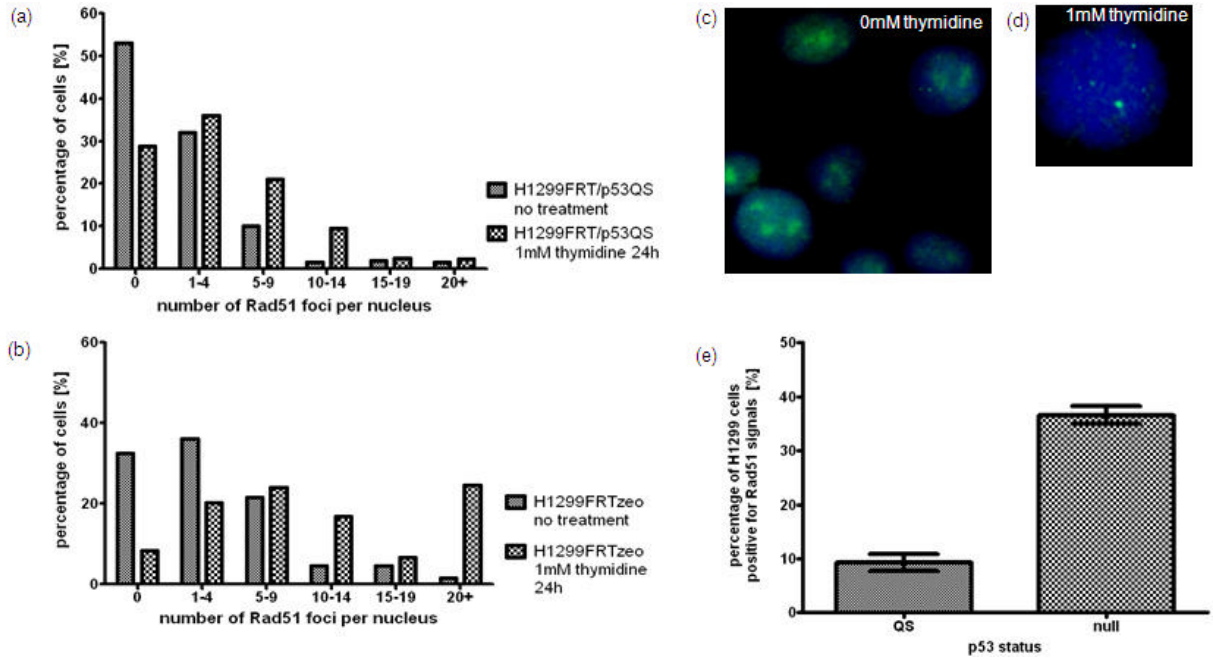

Fig. 4.3: Rad51 foci in H1299FRT/p53QS and H1299FRTzeo cells after 24 hours treatment with thymidine at 1mM (n = 2). (a) Percentage of untreated H1299FRT/p53QS cells that exhibit nuclear Rad51 foci and after the treatment with thymidine (1mM, 24h). (b) Percentage of untreated H1299FRTzeo cells that exhibit nuclear Rad51 foci and after the treatment with thymidine (1mM, 24h). (c) Photograph of H1299FRTzeo control cells with three foci in the cell in the right corner and 2 foci in the cell in the left corner. Other cells are without foci. (d) Photograph of a H1299FRTzeo cell after the treatment with thymidine (1mM, 24h) with five foci. (e) Rad51 foci in H1299FRT/p53QS and H1299FRTzeo cells after 24 hours treatment with thymidine at 1mM showing cells with ten and more foci per nucleus (n = 2). The graph shows the percentages of cells being positive for Rad51 signals (10 or more foci per nucleus) in both cell lines, control subtracted.

In the former two experiments we reproduced the data that p53-null cells show a lower percentage of Rad51 foci per nucleus than wt p53 and p53QS expressing cells after the treatment with thymidine (Bishop et al., 2003; Sengupta and Harris, 2005; Gatz and Wiesmüller, 2006; Keimling and Wiesmüller, 2009). P53QS has a transcription activity that is only 25 - 30% as the one of wt p53 (Romanova et al., 2004). Even though the transcription factor activity is very low in p53QS cells, we see a clear suppression of the HR activity in these cells if compared to p53-null cells. We conclude that the transcription factor activity of wt p53 cannot be the essential factor of the suppression of the HR activity by wt p53.

4.3 THE TRANSIENT TRANSFECTION OF A549/P53M237I AND H1299FRT/P53M237I: INDICATION OF P53 M237I'S GAIN-OF-FUNCTION

We established A549/p53M237I and H1299FRT/p53M237I cells with transient transfection. Directly after colonies had grown in Petri dishes, cells were used for immunofluorescence microscopy. After transient transfection and treatment with thymidine (5mM, 24h) Rad51 foci were counted.

Shown in fig. 4.4, after transient transfection with p53M237I 2% of A549 cells showed ten or more foci compared to 18% of H1299 cells. After the treatment with thymidine (5mM, 24h), the percentages of cells having ten or more Rad51 foci per nucleus increased to 18% in A549/p53M237I compared to 92% in H1299FRT/p53M23I cells.

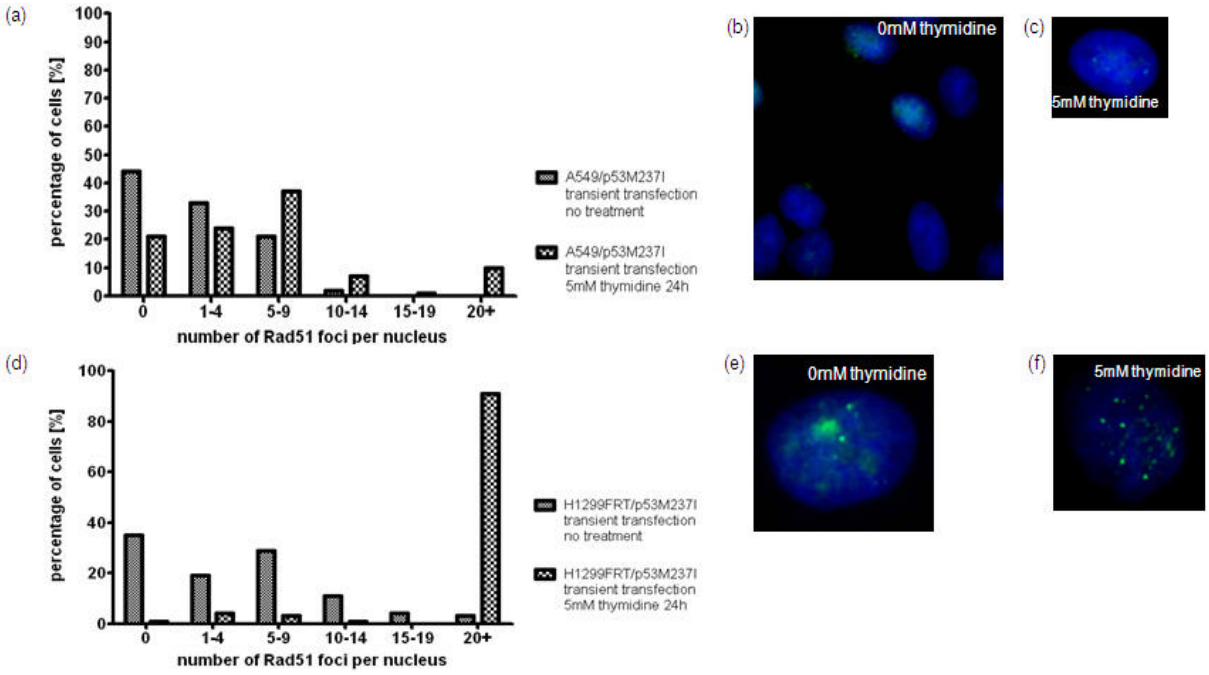

Fig. 4.4: Rad51 foci in A549/p53M237I and H1299FRT/p53M237I cells following transient transfection after the treatment with thymidine (5mM, 24h) (n = 1). (a) Percentage of untreated A549/p53-237 cells that exhibit nuclear Rad51 foci and after the treatment with thymidine (5mM, 24h). (b) Photograph of A549/p53M237I control cells without foci. (c) A549/p53M237I cell after the treatment with thymidine (5mM, 24h) with 3 foci. (d) Percentage of untreated H1299FRT/p53-237 cells that exhibit nuclear Rad51 foci and after the treatment with thymidine (5mM, 24h). (e) Photograph of an H1299FRT/p53M237I control cell with 2 foci. (f) H1299FRT/p53M237I cell after the treatment with thymidine (5mM, 24h) with more than 20 foci.

Gain-of-function is defined as a higher HR activity in p53 M237I mutant cells as in p53-null cells. The big amount of H1299FRT/p53M237I cells positive for Rad51 signaling is rather due to a gain-of function of p53 M237I than due to dominant-

negative properties. To prove our hypothesis right we conducted a further experiment comparing stable transfected p53 M237I mutant cells to p53-null and wt p53 expressing cells.

4.4 WESTERN BLOT OF P53M237I-MUTANTS

Lysates of the H1299FRT/p53M237I cell lines were blotted in a western blot, shown in fig. 4.5. Beside the single clone derived cell lines, we additionally used lysates of H1299FRTzeo and the H1299 pooled cell line. Pooled cell lines derived from different cells, not all cells were identical. To obtain a pooled population a whole Petri dish was trypsinized.

As expected, every cell line except for the H1299FRTzeo showed a band at 53kDa, so every cell line except for H1299FRTzeo securely expressed the p53 mutant M237I.

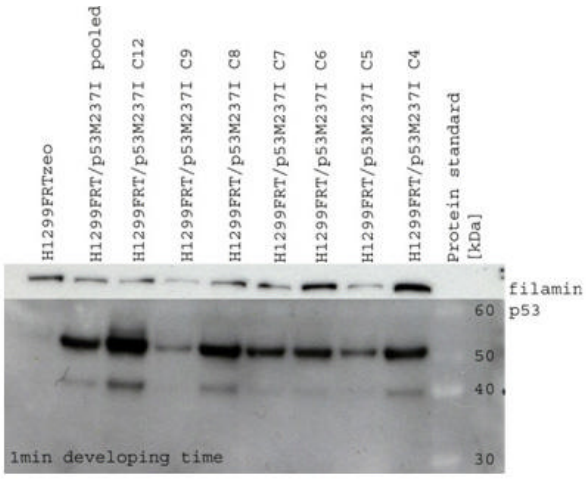

Fig. 4.5: Western blot of p53M237I cell lines. 1min developing time, staining with filamin (upper half) and anti-p53 (lower half). From left to right, lanes show the following cell lines: H1299FRTzeo, H1299FRT/p53M237I pooled, H1299FRT/p53M237I C12, C9, C8, C7, C6, C5 and C4. The lane on the right shows the protein standard [kDa]. Antibodies to filamin served as a loading control.

4.5 RELATIVE EXPRESSION LEVELS OF P53 IN H1299FRT/P53M237I MUTANT CELL LINES

Based on the Western Blot, relative expression levels of p53M237I in the different H1299FRT/p53M237I cell lines were calculated. H1299FRT/p53M237I C12 showed the highest expression (4.16), followed by H1299FRT/p53M237I C8 (2.53), pooled (2.44), C7 (2.18), C5 (1.92), C9 (1.85), C6 (1.22) and C4 (1.00), shown in fig. 4.6.

The expression level is normalized on the cell line clone C4, the clone with the lowest expression level.

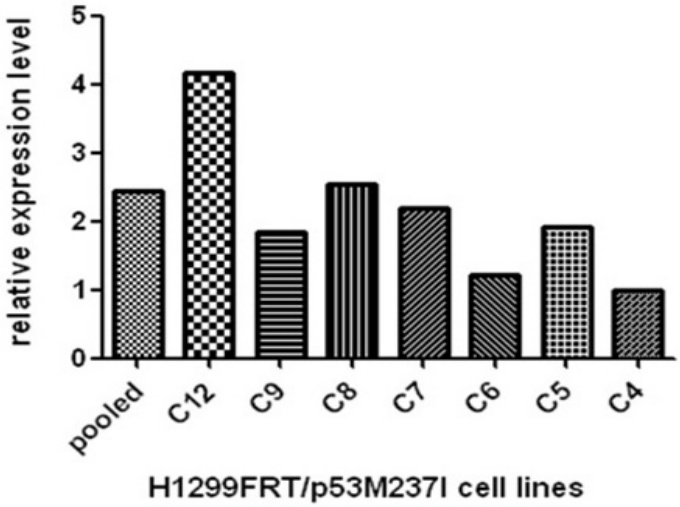

Fig. 4.6: Relative p53 expression levels in different H1299FRT/p53M237I cell lines. The relative expression level of p53 in different cell lines was calculated based on the western blot (Fig. 4.5). Expression level 1 is normalized on the lowest level of expression: C4 = 1.

4.6 P53 M237I IS A GAIN-OF-FUNCTION MUTANT

To confirm p53 M237I is a gain-of-function mutant we compared H1299 cell lines that do not express p53 (H1299FRTzeo) and p53QS expressing cells (H1299FRT/p53M237I) to cells that express the p53 mutant M237I (H1299FRT/p53M237I pooled, H1299FRT/p53M237I C6 and C9) after the treatment with thymidine (1mM, 24h), shown in fig. 4.7.

Shown in fig. 4.7 (a), untreated H1299FRT/p53QS cells similar in its suppression of HR activity as wt p53 showed more than ten Rad51 foci per nucleus in 5%, increasing to 22.5% after the treatment with thymidine (1mM, 24h).
11.5% of untreated H1299FRTzeo cells expressing no p53 showed ten or more Rad51 foci per nucleus. After the treatment with thymidine (1mM, 24h) the percentage of cells with ten or more Rad51 foci per nucleus increased to 53.85% (shown in fig. 4.7 (b)).
Comparing H1299FRTzeo to H1299FRT/p53QS cells we confirmed that p53QS mutant cells, similar in their suppression of HR activity to wt p53 cells, showed a lower HR activity than p53-null H1299FRTzeo cells: p53QS suppressed the HR activity similar to wt p53.

To confirm p53M237I being a gain-of-function mutant we treated three more cell lines (H1299FRT/p53M237I pooled, H1299FRT/p53M237I C6 and C9) with thymidine (1mM, 24h).

Shown in fig. 4.7 (c)-(e), 21% of untreated H1299FRT/p53M237I cells of the pooled cell line, 7.7% of the C6 cell line and 12% of the C9 cell line showed ten or more Rad51 foci per nucleus. In all three cell lines the percentage of cells with ten or more Rad51 foci per nucleus increased after the treatment with thymidine (1mM, 24h): to 79% in the pooled, to 69% in the C6 and to 71% in the C9 H1299FRT/p53M237I cell line.

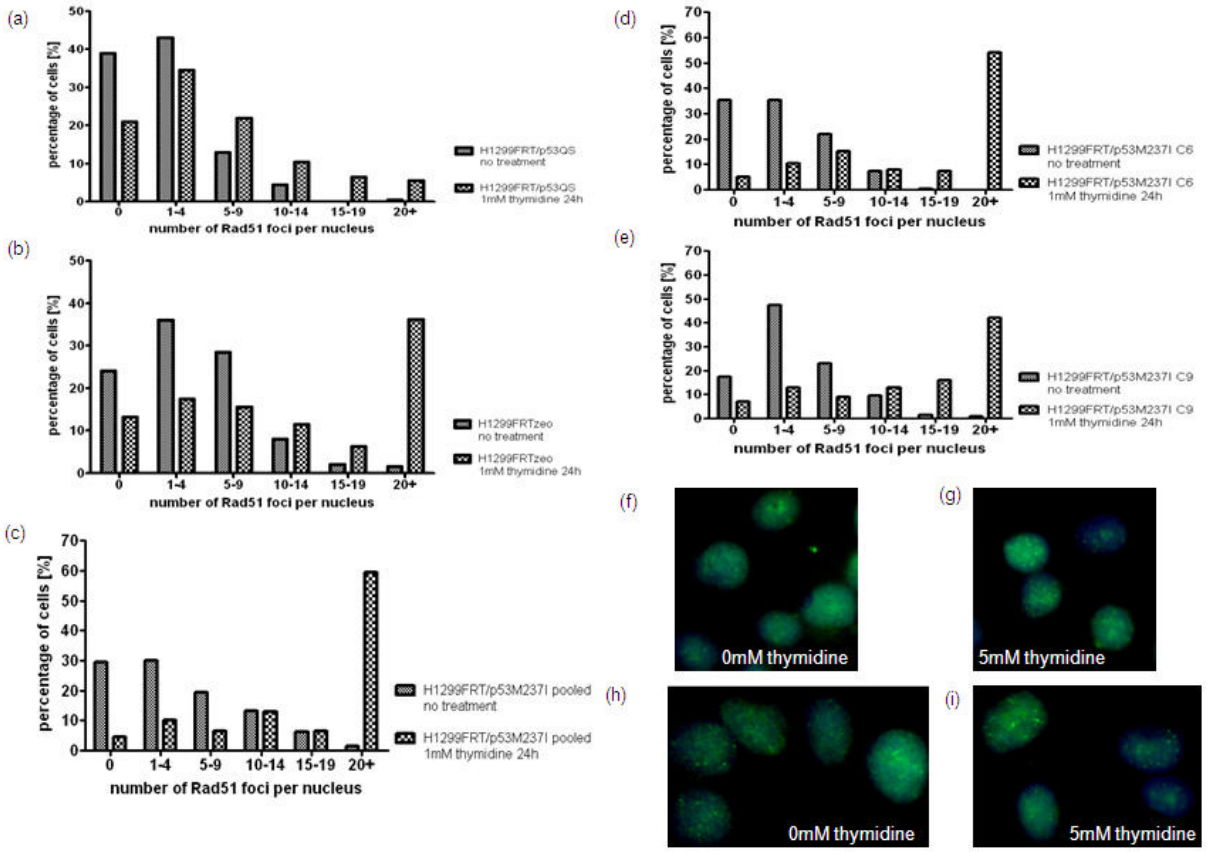

Fig. 4.7: Rad51 foci in H1299FRT/p53QS, H1299FRTzeo, H1299FRT/p53M237I pooled, H1299FRT/p53M237I C6 and H1299FRT/p53M237I C9 cells after 24 hours treatment with thymidine at 1mM (n = 2). (a) Percentage of untreated H1299FRT/p53QS cells that exhibit nuclear Rad51 foci and after the treatment with thymidine (1mM, 24h). (b) Percentage of untreated H1299FRTzeo cells that exhibit nuclear Rad51 foci and after the treatment with thymidine (1mM, 24h). (c) Percentage of untreated H1299FRT/p53M237I pooled cells that exhibit nuclear Rad51 foci and after the treatment with thymidine (1mM, 24h). (d) Percentage of untreated H1299FRT/p53M237I C6 cells that exhibit nuclear Rad51 foci and after the treatment with thymidine (1mM, 24h). (e) Percentage of untreated H1299FRT/p53M237I C9 cells that exhibit nuclear Rad51 foci and after the treatment with thymidine (1mM, 24h). (f) Photograph of an untreated H1299FRT/p53M237I pooled control cell without foci. (g) H1299FRT/p53M237I pooled cells after the treatment with thymidine (1mM, 24h) with 20 or more foci on the left side of the image. (h) Photograph of H1299FRT/p53M237I C9 control cells with no cell having ten or more foci. (i) H1299FRTp53M237I C9 cells after the treatment with thymidine (1mM, 24h) with every cell having five (left lower corner) until 20 or more foci (left upper corner).

In summary, comparing H1299FRT/p53QS (p53QS), H1299FRTzeo (p53-null) and H1299FRT/p53M237I pooled, C6 and C9 (p53M237I) with ten and more foci per nucleus, H1299FRT/p53M237I C6 cells showed the highest percentage of positive cells (62%), followed by H1299FRT/p53M237I C9 (59%) and H1299FRT/p53M237I pooled cells (58%). H1299FRTzeo cells showed a higher percentage of positive cells (42%) than H1299FRT/p53QS (18%), but at least 16% less than all the p53M237I-

mutant cell lines. All three cell lines expressing the p53M237I mutant showed more Rad51 foci per nucleus than p53QS expressing or p53-null cells (shown in fig. 4.8).

As gain-of-function is defined as a higher HR activity than in p53-null cells, our result is compatible with p53 mutant M237I being a gain-of-function mutant.

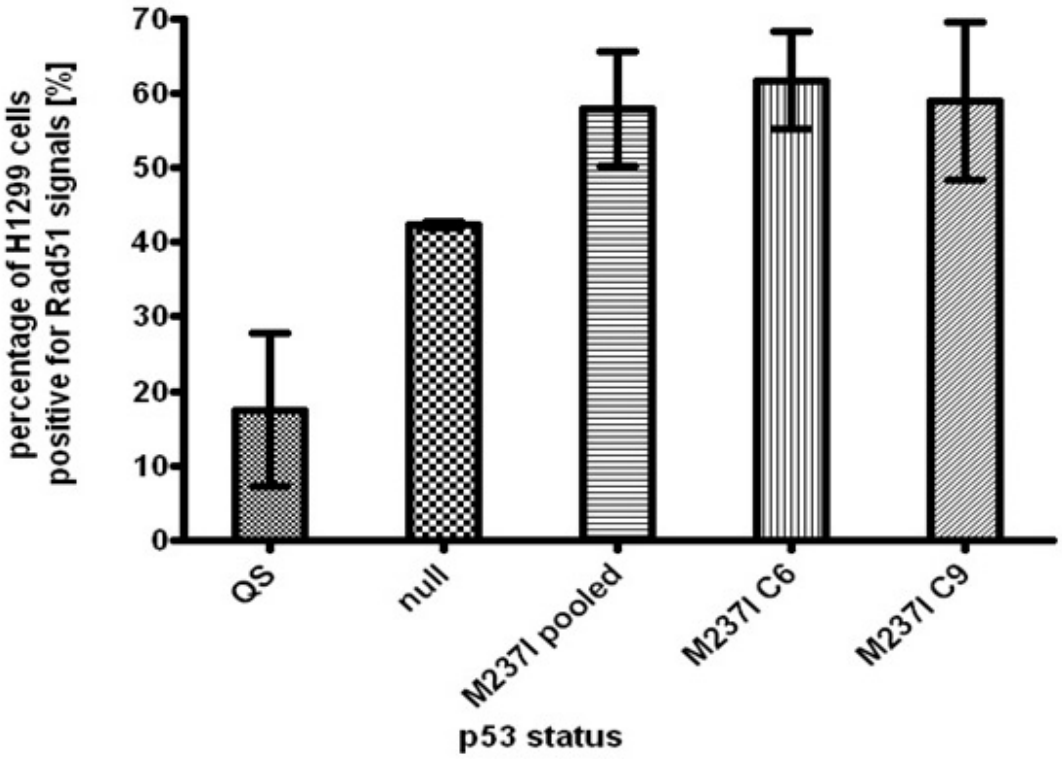

Fig. 4.8: Rad51 foci in H1299FRT/p53M237I cell lines after 24 hours treatment with thymidine at 1mM showing the percentages of cells with ten or more foci per nucleus (n = 2). The graph shows the percentages of cells being positive for Rad51 signals (10 or more foci per nucleus) in all H1299FRT/p53M237I cell lines, control subtracted.

4.7 DSBS IN A549 AND H1299 CELL LINES

The mechanism for the higher number of Rad51 foci in p53 M237I mutant expressing cells compared to p53-null cells is unclear. We hypothesized, the higher HR activity being caused by a higher number of DSBs. We therefore stained H1299FRT/p53QS, H1299FRTzeo and H1299FRT/p53QM cells for gamma-H2AX foci per nucleus before and after the treatment with thymidine (5mM, 5h).

H1299FRT/p53QM cells have a p53QS mutation and an additional N-terminal mutation in the RPA-binding domain (W53S/F54S) that abrogates regulation of HR.

Without any treatment and after the treatment with thymidine (5mM, 5h) virtually all cells showed more than 20 foci with no differences between strains, shown in fig. 4.9. We saw no difference in the gamma-H2AX staining in the different H1299 cell lines.

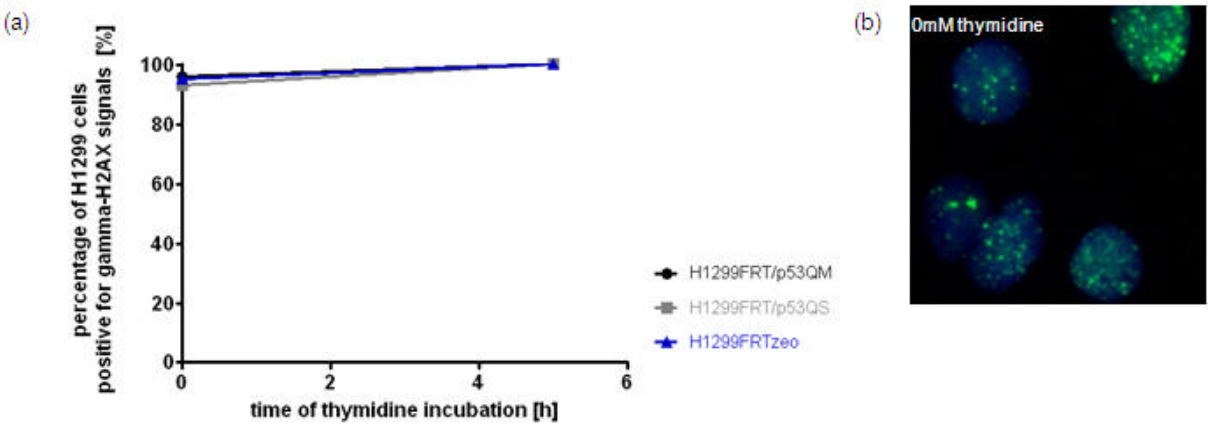

Fig. 4.9: Gamma-H2AX foci in H1299FRT/p53QM, H1299FRT/p53QS and H1299FRTzeo cells after 5 hours treatment with thymidine at 5mM with cells having 20 and more foci per nucleus (n = 1). (a) Percentage of untreated H1299FRT/p53QS, H1299FRT/p53QM and H1299FRTzeo cells that exhibit nuclear gamma-H2AX signals and after the treatment with thymidine (5mM, 0-6h). (b) Photograph of H1299FRTzeo control cells with more than 20 gamma-H2AX foci.

The staining for gamma-H2AX in H1299 cell lines after the thymidine treatment did not show any differences between the cell lines because of the high background staining with gamma-H2AX in H1299 cells. Therefore we stained for gamma-H2AX in different cell lines, A549 cell lines, treated with hydroxyurea (1mM, 24 hours), shown in fig. 4.10.

8% of untreated A549cDNA and 30% of A549/p53-273L cells had ten or more foci per nucleus. After the treatment with hydroxyurea (1mM, 24h) the percentage of cells with ten or more foci per nucleus increased to 18.5% in A549cDNA and to 47.5% in A549/p53-273L cells.

Comparing cells with ten and more foci per nucleus after the treatment with hydroxyurea (1mM, 24h) we could show a difference of gamma-H2AX foci in A549 cells differing in p53 status: 17% of A549/p53-273L cells were positive for gamma-H2AX foci signaling in comparison to only 11% of A549cDNA cells. A549/p53-273L cells expressing the dominant-negative p53 mutant 273L showed a 6% higher percentage of gamma-H2AX foci signaling cells than A549cDNA cells expressing wt p53 (shown in fig. 4.10 (c)).

In summary, we observed a higher number of Rad51 and gamma-H2AX foci in A549 cells expressing the dominant-negative p53 mutant 273L in comparison to cells expressing wt p53. The higher HR activity seen in dominant-negative p53 mutant 273L cells could be due to a higher number of DSBs in those cells.

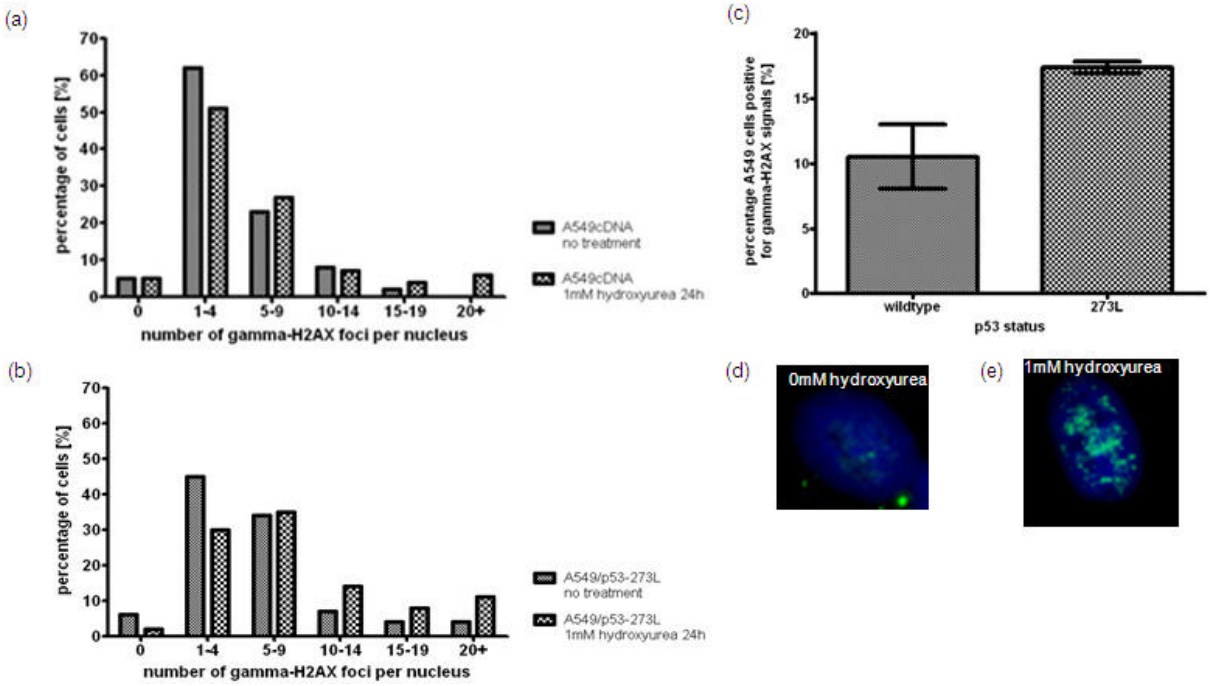

Fig. 4.10: Gamma-H2AX foci in A549cDNA and A549/p53-273L cells after 24 hours treatment with hydroxyurea at 1mM (n = 2). (a) Percentage of untreated A549cDNA cells that exhibit nuclear gamma-H2AX foci and after the treatment with hydroxyurea (1mM, 24h). (b) Percentage of untreated A549/p53-273L cells that exhibit nuclear gamma-H2AX foci and after the treatment with hydroxyurea (1mM, 24h). (c) Gamma-H2AX foci in A549 cell lines after the 24 hours treatment with hydroxyurea at 1mM with percentages showing cells with ten or more foci per nucleus (n = 2). The graph shows the percentages of cells being positive for gamma-H2AX signals (10 or more foci per nucleus) in both cell lines, control subtracted. (d) Photograph of an A549/p53-273Lcontrol cell without foci. (e) A549/p53-273L cell after the treatment with hydroxyurea at 1mM for 24h.

In the following experiment we stained for gamma-H2AX foci in A549cDNA and A549/p53-273L cells again but after the treatment with thymidine (5mM, 24h). Thymidine was reported to not cause DSBs (Lundin et al., 2002).

19% of untreated A549cDNA cells had ten or more gamma-H2AX foci per nucleus; in A549/p53-273L the percentage of untreated cells with ten or more gamma-H2AX foci per nucleus was 27.5%. After the treatment with thymidine (5mM, 24h) the percentage of treated cells with ten or more foci per nucleus increased to 28.5% in A549cDNA and 51.5% in A549/p53-273L cells (shown in fig. 4.11).

Comparing A549/p53-273L and A549cDNA with ten and more foci per nucleus after the treatment with thymidine (5mM, 24h), 24% of A549/p53-273L, whereas only 9.5% of A549cDNA were positive for gamma-H2AX foci signaling (shown in fig. 4.11 (e)). We concluded that thymidine causes more DSBs in p53-273L than in wt p53 expressing cells.

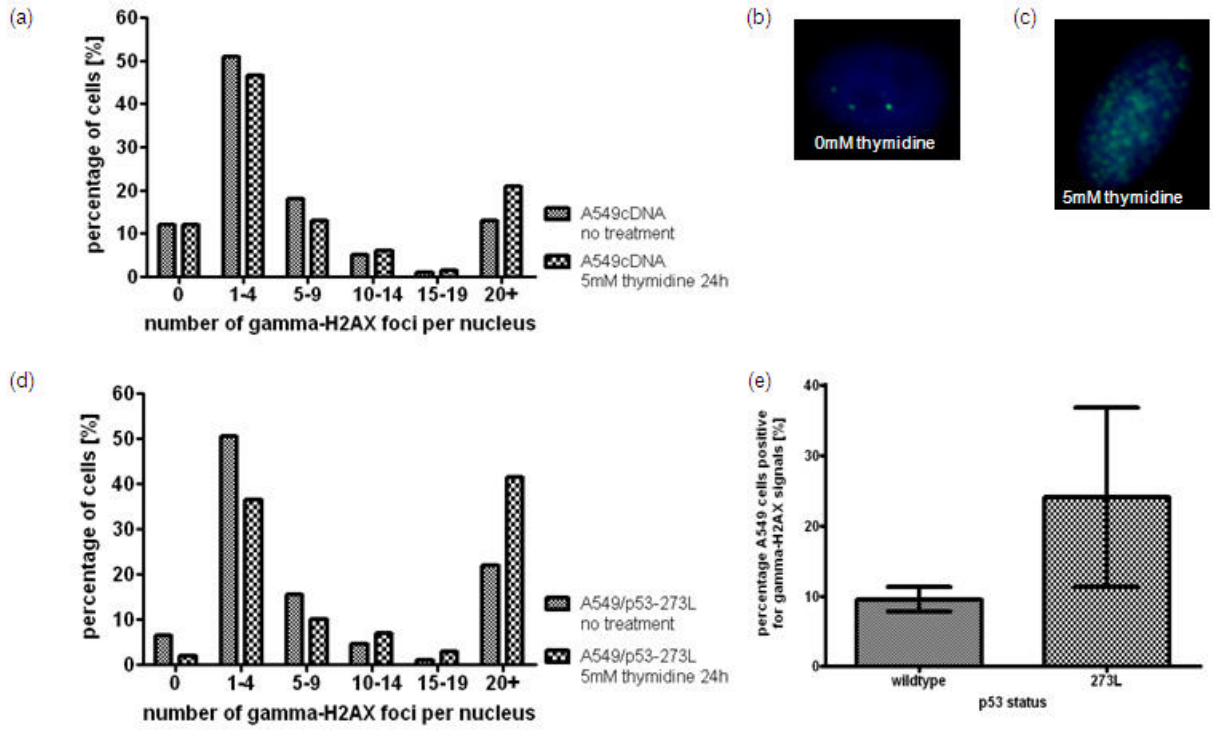

Fig. 4.11: Gamma-H2AX foci in A549cDNA and A549/p53-273L after the treatment with thymidine (5mM, 24h) (n = 2). (a) Percentage of untreated A549cDNA cells that exhibit nuclear gamma-H2AX foci and after the treatment with thymidine (5mM, 24h). (b) Photograph of an A549cDNA control cells with 3 gamma-H2AX foci. (c) A549cDNA cells after the treatment with thymidine (5mM, 24h) with 20 or more gamma-H2AX foci. (d) Percentage of untreated A549/p53-273L cells that exhibit nuclear gamma-H2AX foci and after the treatment with thymidine (5mM, 24h). (e) Gamma-H2AX foci in A549cDNA and A549/p53-273L cells after the treatment with thymidine (5mM, 24h) showing the percentages of cells with 10 and more foci per nucleus (n = 2). The graph shows the percentages of cells being positive for gamma-H2AX signals (10 or more foci per nucleus) in both cell lines, control subtracted.

4.8 P53-MUTANT M237I CELLS HAVE MORE DSBS THAN WT P53 AND P53 QS CELLS AFTER 24 HOURS TREATMENT WITH HYDROXYUREA AT 1MM

As the gamma-H2AX staining in H1299 cells did not deliver any results concerning the DSB status because of the high background staining, we stained

H1299FRT/p53QS, H1299FRTzeo and H1299FRT/p53M237I cells for 53BP1. 53BP1 (p53 binding-protein 1) is also known as a marker for DSBs which becomes phosphorylated by the ATM (ataxia teleangiectasia mutated) kinase after DSBs. It is a downstream signal of histone H2AX in response to DNA damage (Fernandez-Capetillo et al., 2002).

Comparing cells with ten and more foci per nucleus after the treatment with hydroxyurea (1mM) we did not see any significant differences between the cell lines H1299FRT/p53QS, H1299FRTzeo and H1299FRT/p53M237I pooled (shown in fig. 4.12). The highest percentage of 53BP1 signals showed H1299FRT/p53M237I pooled cells with 8% of cells being positive for 53BP1 signals after the treatment with hydroxyurea (1mM, 24 hours) compared to 3.5% in H1299FRTzeo and H1299FRT/p53QS cell lines. We conclude that hydroxyurea causes DSBs marked by 53BP1 in all three H1299 cell lines but at low percentages.

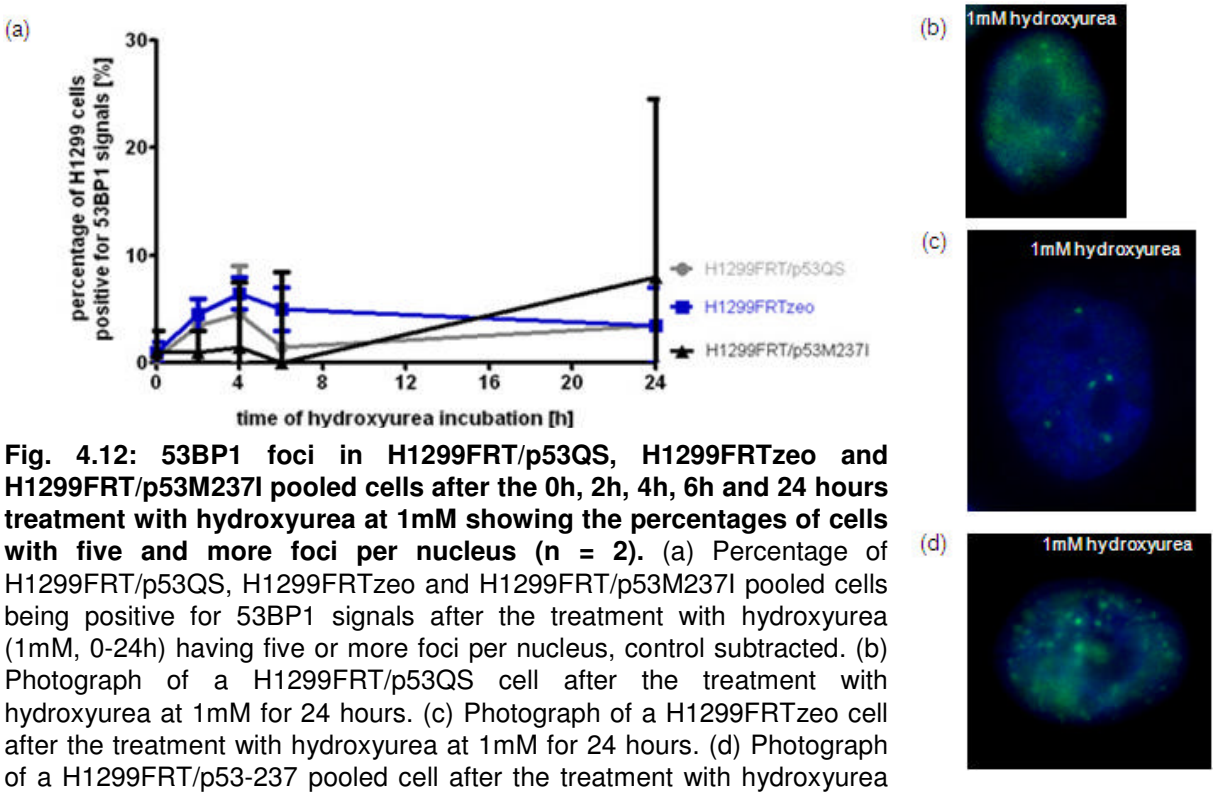

Fig. 4.12: 53BP1 foci in H1299FRT/p53QS, H1299FRTzeo and H1299FRT/p53M237I pooled cells after the 0h, 2h, 4h, 6h and 24 hours treatment with hydroxyurea at 1mM showing the percentages of cells with five and more foci per nucleus (n = 2). (a) Percentage of H1299FRT/p53QS, H1299FRTzeo and H1299FRT/p53M237I pooled cells being positive for 53BP1 signals after the treatment with hydroxyurea (1mM, 0-24h) having five or more foci per nucleus, control subtracted. (b) Photograph of a H1299FRT/p53QS cell after the treatment with hydroxyurea at 1mM for 24 hours. (c) Photograph of a H1299FRTzeo cell after the treatment with hydroxyurea at 1mM for 24 hours. (d) Photograph of a H1299FRT/p53-237 pooled cell after the treatment with hydroxyurea at 1mM for 24 hours.

4.9 RPA FOCI FORMATION IN H1299 CELL LINES AFTER THE TREATMENT WITH THYMIDINE AT 5MM

P53 is known for its suppression of HR in a variety of human cell lines (Willers et al., 2000; Akyüz et al., 2002; Janz and Wiesmüller, 2002; Boehden et al., 2003). The

mechanism of the suppression of HR by p53 has not already been clarified. There are probably multiple mechanisms how p53 inhibits HR.
RPA (Replication Protein A) is a single-stranded (ss) DNA-binding protein involved in replication and HR (Golub et al., 1998; Iftode et al., 1999). P53QS is similar to wt p53 in binding RPA and suppressing HR (Romanova et al., 2004).

We stained for RPA foci in H1299FRT/p53QS, H1299FRTzeo and H1299FRT/p53M237I cells after the treatment with thymidine (5mM, 0h, 2h, 4h, 6h and 24h), shown in fig. 4.13.
The percentages of cells being positive for RPA foci signaling in all three cell lines H1299FRT/p53QS, H1299FRTzeo and H1299FRT/p53M237I increased from the 0 to 24 hours time point after the treatment with thymidine (5mM).
As RPA foci are replication foci, differences between the cell lines in between the 0 and 24 hours time point could be due to the difference in proliferation instead of being due to the different p53 status in the cell lines. Sirbu et al. (2011) showed similar cell cycle profiles in response to thymidine treatment for p53-null and p53QS cell lines. We therefore concluded different cell cycle profiles of the cell lines were not the main cause of the different number of RPA foci between the H1299 cell lines in between the 0 and 24 hours time point.

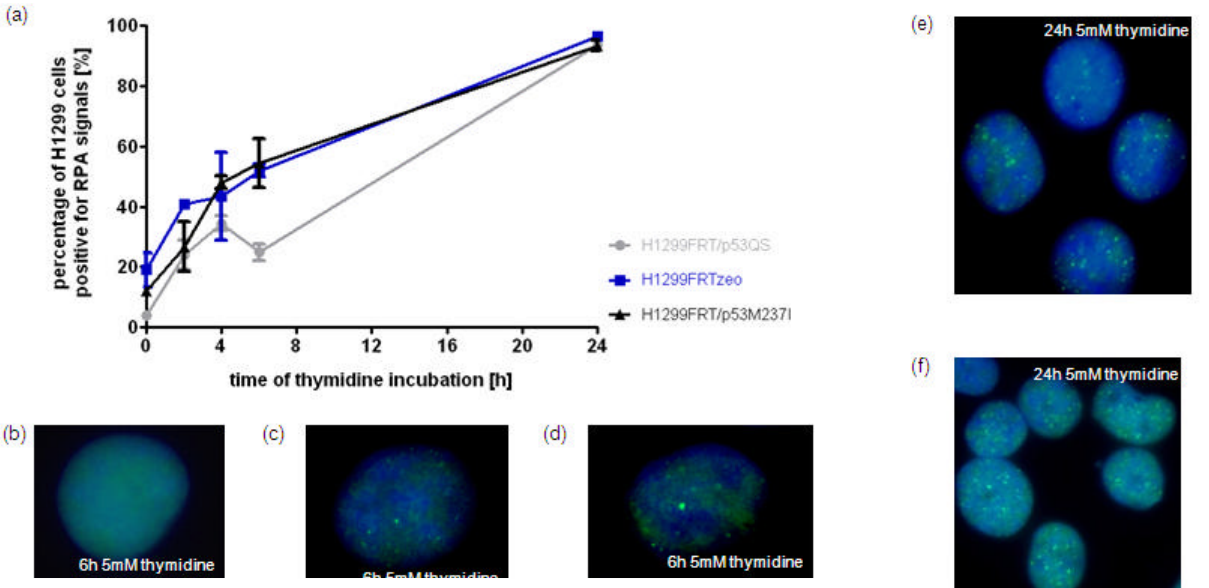

Fig. 4.13: RPA foci in H1299FRT/p53QS, H1299FRTzeo and H1299FRT/p53M237I pooled cells after 0h, 2h, 4h, 6h and 24 hours treatment with thymidine at 5mM showing percentages of cells with ten and more foci per nucleus (n = 2). (a) Percentages of H1299FRT/p53QS, H1299FRTzeo and H1299FRT/p53M237I pooled cells being positive for RPA signals having ten or more foci per nucleus, control subtracted. (b) Photograph of a H1299FRT/p53QS cell after the treatment with thymidine for 6h at 5mM without foci. (c) Photograph of a H1299FRTzeo cell after the treatment with thymidine at 5mM for 6h with 13 foci. (d) Photograph of a H1299FRT/p53M237I pooled cell after the treatment with thymidine at 5mM for 6h with 11 foci. (e) Photograph of H1299FRT/p53QS cells after the treatment with thymidine at 5mM for 24 hours.(f) Photograph of H1299FRTzeo cells after the treatment with thymidine at 5mM for 24 hours. (g) Photograph of H1299FRT/p53M237I pooled cells after the treatment with thymidine at 5mM for 24 hours.

5 DISCUSSION

5.1 P53QS MEDIATES THE SUPPRESSION OF THE HR ACTIVITY

Several groups reported about the suppression of HR by wt p53. In p53-null cells the HR activity was higher than in wt p53 expressing cells (Gatz et al., 2000; Janz and Wiesmüller, 2002). In H1299 cells we measured Rad51 foci in cells expressing the mutant p53QS. Using H1299FRT/p53QS cells that carry the QS-mutation (L22Q/W23S) which reduces transcriptional activity to 25 – 30% of wt p53 (Willers et al., 2000; Boehden et al., 2003; Romanova et al., 2004), we saw a clear suppression of the HR activity after the treatment with thymidine at 1mM and 5mM (24h) in cells expressing p53QS (shown in fig. 4.2 and 4.3). We concluded that the transcription factor activity of p53 cannot be the essential factor of the suppression of the HR activity mediated by wt p53.

The wt p53 transcription factor activity is important for the G1 arrest and apoptosis as wt p53 activates key-proteins of these pathways, such as p21 that is important to the G1 arrest (Willers et al., 2000; Boulon et al., 2010). If p21 is not expressed under the influence of p53 mutants the suppression of the HR still takes place; the HR suppression is independent of the G1 cell cycle arrest (Willers et al., 2000).

The question to ask is whether we see a higher HR activity in p53-null than in wt p53 expressing cells because wt p53 normally induces G1-arrest or apoptosis in damaged cells? Willers and colleagues (2000) found that growth characteristics, transfection frequencies and plating efficiencies showed no significant differences in their data and concluded apoptosis being unlikely responsible for the differences in the recombination frequencies. Sirbu et al. (2011) showed similar cell cycle profiles in response to thymidine treatment for p53-null and p53QS cell lines. We concluded that our results are not mainly due to different cell cycle distributions.

The dominant-negative p53 mutant 273L was shown to not suppress the HR activity (Romanova et al., 2004) which we could reproduce in A549 cells expressing the p53 mutant 273L that showed a higher number of Rad51 foci per nucleus than wt p53 expressing cells after the treatment with thymidine (5mM, 24h), shown in fig. 4.1.

5.2 MUTANT P53 M237I – PRESUMABLE A GAIN-OF-FUNCTION MUTANT

In the transient transfected A549/p53M237I and H1299FRT/p53M237I cells we counted very high numbers of cells with ten and more Rad51 foci per nucleus (shown in fig. 4.4). Without comparing wt p53 cells we could not prove the mutant p53M237I being responsible for these high Rad51 foci level. We conducted a stable transfection to compare mutant p53 M237I expressing cells to wt p53 expressing cells.

Xia et al. (1994; 1995; 1997) reported about a 7-fold increased recombination activity in WTK1 (p53 mutant M237I) cells compared to TK6 (wt p53) cells (Xia et al., 1995). They also found increased spontaneous and x-ray induced mutation frequencies in mutant p53 M237I compared to wt p53 expressing cells. Compared to TK6 (wt p53) cells WTK1 (p53 M237I) cells showed apoptosis delayed by three days (Xia et al., 1995). Mutant p53 M237I was found to be a hyper-recombination phenotype. If the p53 mutant M237I was a gain-of-function mutant remained unclear. Chuang et al. (1999) reported p53 mutant M237I cells being less sensitive to radiation induced cytotoxicity and being more sensitive to the induction of mutations of the thymidine kinase (TK) and the HPRT loci than wt p53 expressing cells.

The comparison of H1299FRT/p53QS and H1299FRTzeo cells with ten and more Rad51 foci per nucleus after the treatment with thymidine (1mM, 24h), showed a difference in cells being positive for Rad51 foci signaling of 25% (shown in fig. 4.7) which was similar to the former results of 27% (1mM thymidine, 24h) shown in fig. 4.3. The number of cells with 20 or more Rad51 foci after the treatment with thymidine (5mM, 24h) shown in fig. 4.2 (e) showed a difference between H1299FRT/p53QS and H1299FRTzeo cells of 51%.
All cell lines expressing the p53-mutant M237I conducted by stable transfection showed higher percentages of cells being positive for Rad51 foci signaling than H1299FRT/p53QS or H1299FRTzeo cells, shown in fig. 4.8. Less than 16 - 20% of the p53-null cells were positive for Rad51 foci signaling in comparison to p53M237I expressing cells.

The increase of HR activity in p53 M237I mutant cells would be compatible with a gain-of-function of mutant p53M237I. P53 mutant M237I could increase the HR but there is also the possibility that we see more Rad51 foci because of more DSBs in these p53 mutant M237I expressing cells.

5.3 HIGHER HR ACTIVITY CAUSED BY A HIGHER NUMBER OF DSBS?

We wanted to prove the hypothesis that the higher number of Rad51 foci in H1299FRT/p53M237I cells is caused by a higher number of DSBs.

In our experiments we treated cells with the replication elongation inhibitors hydroxyurea and thymidine.

Thymidine is a replication elongation inhibitor that depletes cells of the deoxyribonucleoside triphosphate dCTP. Cells slow down in their DNA replication activity and the retardation of replication delivers substrates for recombinational repair. The so called chicken foot formation (shown in fig. 2.5 (e)) is a result of the fork regression. In contrast to hydroxyurea, the DNA damage following thymidine treatment is repaired by HR only, and thymidine does not cause DSBs (Lundin et al., 2002). Lundin et al. (2002) hypothesized that the replication complex does not dissociate from the replication fork, the replication fork does not stall and no DNA DSBs result because nucleotides are still incorporated in the DNA after the thymidine treatment.

Hydroxyurea is a DNA replication elongation inhibitor that depletes cells of several deoxyribonucleoside triphosphates which leads to replication fork arrest (Lundin et al., 2002; Hartlerode and Scully, 2009). Stalled replication forks lead to DNA DSBs (Lundin et al., 2002; Bonner et al., 2008) that are repaired by HR. In S-phase hydroxyurea induces HR, visibly by Rad51 foci induction (Lundin et al., 2002).

Both hydroxyurea and thymidine are proposed to be cytotoxic by causing lesions that accumulate at replication forks (Lundin et al., 2002). After the treatment with thymidine as well as after the treatment with hydroxyurea subnuclear Rad51 foci are formed and a suppression of the formation of those Rad51 foci is seen in p53QS expressing cells, compared to p53-null cells (Sirbu et al., 2011).

We saw no differences and no effect in the gamma-H2AX staining between the H1299 cell lines after the treatment with thymidine at 5mM (shown in fig. 4.9) which is according to former results (Lundin et al., 2002). The gamma-H2AX background staining in H1299 cells was too high to measure an additional effect of thymidine on DSBs in those cells. We therefore had to use two different methods: First, we stained A549 cells after a thymidine (5mM, 24h) and after a hydroxyurea (1mM, 24h) treatment for gamma-H2AX. Second, we measured 53BPI foci in H1299 cells.

First, comparing A549/p53-273L and A549cDNA with ten and more foci per nucleus after the treatment with thymidine (5mM, 24h), 24% of A549/p53-273L, whereas only 9.5% of A549cDNA were positive for gamma-H2AX foci signaling (shown in fig. 4.11 (e)). We concluded that thymidine causes more DSBs in p53-273L than in wt p53 expressing cells. Lundin et al. (2002) did not measure DSBs after the thymidine treatment. The higher number of Rad51 foci that we saw in A549/p53-273L cells (shown in fig. 4.1) could be caused by a higher number of DSBs.

Comparing A549/p53-273L and A549cDNA cells being positive for gamma-H2AX foci signaling after the hydroxyurea treatment, we saw a 6% higher fraction of A549/p53-273L cells positive for gamma-H2AX compared to A549cDNA cells (shown in fig. 4.10 (c)). We saw a similar situation in Rad51 foci staining after the treatment with thymidine (5mM, 24h) with the dominant-negative p53-273L mutant expressing cells showing 8% more cells being positive for Rad51 signaling compared to wt p53 expressing A549cDNA cells (fig. 4.1).
The relative difference between the two cell lines in the gamma-H2AX compared to the Rad51 foci staining was similar, but real numbers of cells being positive for gamma-H2AX staining compared to Rad51 staining were different.

As another method to prove our hypothesis that we see more Rad51 foci because of more DSBs we stained for 53BP1 in H1299 cells. 53BP1 is a marker for DSBs which becomes phosphorylated by ATM. It is a downstream signal of histone H2AX in response to DNA damage (Fernandez-Capetillo et al., 2002).

Staining for 53BP1 in H1299 cell lines after the treatment with hydroxyurea at 1mM, we saw cells being positive for 53BP1 signaling in every H1299 cell line (H1299FRTzeo, H1299FRT/p53QS and H1299FRT/p53M237I pooled) at the 24 hours time point (shown in fig. 4.12) with H1299FRT/p53M237I pooled having the most 53BPI foci. This result is compatible with more Rad51 foci being caused by more DSBs in those cells.

53BP1 and gamma-H2AX are both marker for DSBs that do not always correlate (Marková et al., 2007). In our experiments nearly every H1299 cell showed ten or more gamma-H2AX foci whereas the number of 53BP1 foci was between 0-8%. Gamma-H2AX mediates the recruitment of DNA repair proteins (e.g. 53BP1) to DNA damage. The recruitment is necessary to amplify the DNA damage signals

(Fernandez-Capetillo et al., 2002; Ismail and Hendzel, 2008). 53BP1 is one of the downstream signals of gamma-H2AX (Fernandez-Capetillo et al., 2002; Sonoda et al., 2005).
In our experiments we saw a lot of the DNA damage being marked by gamma-H2AX but a lower percentage of 53BP1 recruitment to the damage. The result with a lower percentage of cells being positive for 53BP1 signaling in comparison to cells being positive for gamma-H2AX foci signaling after hydroxyurea treatment, which is known to mainly cause DSBs, could be due to the fact that gamma-H2AX molecules do not only mark DSBs but form at several more cases than DSB formation, e.g. at single-stranded DNA breaks (Fragkos et al., 2009).

In summary, with gamma-H2AX staining in H1299 cells we could not see an effect of thymidine on the rate of DSBs in those cells. Using another cell line, A549, we could see more gamma-H2AX foci after the thymidine and after the hydroxyurea treatment. Thymidine causing DSBs was not reported by Lundin et al. (2002). Staining for 53BP1 cells showed the highest number for 53BP1 foci in the H1299/FRTp53M237I pooled cells. This result is compatible with a higher number of Rad51 foci in H1299/FRTp53M237I expressing cells being caused by a higher number of DSBs in those cells.

5.4 A POSSIBLE ROLE OF RPA IN THE SUPPRESSION OF HR

Wt p53 is known to bind to RPA and prevents it from ssDNA-binding (Kantake et al., 2003; Romanova et al., 2004). We asked if the mutant p53-M237I does behave different to RPA.

Staining H1299 cells for RPA foci after the treatment with thymidine at 5mM (shown in fig. 4.13) we saw every cells of all three cell lines having ten or more RPA foci at the 24 hours time point.

It exist several possibilities of why we see RPA foci after the thymidine treatment. First possibility is that RPA foci arise from the thymidine treatment itself. Thymidine is a replication elongation inhibitor that synchronizes growing cells in the S phase of the cell cycle (Lundin et al., 2002). RPA is a single-stranded (ss) DNA-binding protein involved in replication and HR (Golub et al., 1998; Iftode et al., 1999) and replication takes place in the S phase of the cell cycle. Therefore the RPA foci could arise

because of the thymidine treatment.
Second, as RPA foci are replication foci, differences between the cell lines could be due to the difference in proliferation instead of being due to the different p53 status in the cell lines. Sirbu et al. (2011) showed similar cell cycle profiles in response to thymidine treatment for p53-null and p53QS cell lines. We therefore concluded different cell cycle profiles of the cell lines were not the main cause of the suppression of RPA foci in H1299FRT/p53QS cells.
Third, RPA could be needed for the suppression of HR by wt p53. RPA and Rad51 co-localize on synapsed axes in meiosis, in damage induced Rad51 foci or after gamma-irradiation in common foci (Golub et al., 1998). Additionally, wt p53 is known to directly bind to RPA's 70kDa subunit preventing RPA from binding to ssDNA in case of spontaneous or DSB-induced HR. The intact binding between wt p53 and RPA seems to be necessary for the suppression of HR by wt p53 (Romanova et al., 2004; Gatz and Wiesmüller, 2006; Reliene et al., 2007). Wt p53's inhibition of RPA binding to ssDNA is independent of the p53 transactivation activity but needs the direct physical interaction with RPA. Mutant p53QS is able to inhibit the RPA binding to ssDNA. The RPA-inhibition is necessary but not sufficient for the HR-inhibition by p53 (Romanova et al., 2004).

In a model proposed by Romanova et al. (2004) the sequestration of RPA from ssDNA subsequently leading to inhibition of Rad51 loading and therefore inhibition of HR was suspected to be part of the suppression of HR by wt p53.

The stabilization of replication forks by wt p53 could also involve the kinase ATR. ATR is activated by DNA damage, e.g. DSBs or replication stress. An increased rate of DSBs during replication was observed in cells with a defective ATR-pathway (Trenz et al., 2006). There is evidence that RPA-coated ssDNA is important to localize the ATR-ATRIP-complex.
Both wt p53 and ATR interact with RPA and the HR suppression by p53QS was shown to be dependent on ATR (Sirbu et al., 2011). Additionally, ATR was shown to be activated by ssDNA framed by a 5'-junction as it is generated during replication fork stalling or end 5'-3' resection at DSBs (Cimprich and Cortez, 2008). It seems likely that both proteins RPA and ATR are involved in the same pathway, e.g. the ATR-checkpoint. Evidence for placing p53 in the ATR-checkpoint was additionally brought by Sirbu et al. (2011) who could show that depleting cells of ATR by siRNA

resulted in a lower suppression of the HR activity in p53QS expressing cells compared to cells with intact ATR kinase activity.

A model compatible with our results is that without p53 or under the influence of the gain-of-function mutant p53M237I the replication forks are not as stabilized as under the influence of wt p53. Subsequently replication forks collapse, we see more DSBs in those cells, represented by more gamma-H2AX and more 53BP1 foci signaling. Those DSBs have to get repaired. Subsequently a higher number of Rad51 foci is observed indicating a higher HR activity in cells expressing the p53 mutant M237I.

5.5 IMPORTANCE OF FINDINGS

It has been reported by numerous groups that inappropriate and elevated levels of HR can lead to genomic alterations (Sengupta et al., 2005; Paulsen and Cimprich, 2007). Genomic alterations can lead to cancer development (Helleday et al., 2007). Brosh and colleagues (2009) postulated the hypothesis that p53 inactivation might be sufficient for tumor initiation at certain tissues while other tissues might additionally require gain-of-function activities of p53 mutants for tumor initiation. P53 mutant M237I possibly causing higher rates of HR could be a candidate for the step towards carcinogenesis in more resistant tissues.

It was reported about a correlation between the overexpression of p53 mutants and the bad prognosis of cancer patients and an association with poor clinical outcome in a growing array of cancer types (Li et al., 1998; Brosh and Rotter, 2009). Additionally it was found p53 mutations being associated with drug resistance in several malignancies and cell lines (Brosh and Rotter, 2009). Chemotherapy in lung-cancer patients with mutant p53 may decrease the survival of these patients (Ma et al., 2008). The knockdown (stable or conditional) of endogenous mutant p53 reduced the proliferation rate and chemoresistance in vitro; nude mice showed a reduced ability to form tumors (Bossi et al., 2006; Bossi et al., 2008). Knowing which p53 mutants are gain-of-function mutants could help in the therapy decision: Therapies based on DSB-induction would not be used.

Studying the p53 mutants in detail is important to get to know the mutant's mechanisms that influence the cells response to anti-cancer therapy. Based on

detailed knowledge about the p53 mutants the next step will be the development of new therapy strategies. The treatment of tumors based on their p53 status will be on step closer to the personalized medicine.

6 SUMMARY

Lung cancer is the number one killer of cancers in women and men. 85% of lung cancer is non-small cell lung cancer (NSCLC). A549 and H1299 are NSCLC cell lines. The worldwide distributions of cancers and the percentage of them containing p53 mutants differ between cancer types. About 50% of NSCLC tumors contain p53 mutations.

Homologous recombination (HR) is an important repair mechanism for DNA double-strand-breaks. Inappropriate and elevated levels of HR can lead to genomic instability which may promote cancer development.

P53 is a protein involved in cell cycle arrest, senescence, apoptosis, differentiation and DNA repair. P53 is the most commonly mutated tumor suppressor gene. A correlation between missing or mutated p53 and the development of cancer is known as well as a correlation between the overexpression of p53-mutants and the bad prognosis of cancer patients.

P53 is known for its direct interactions with components of the HR such as Rad51. Wildtype p53 downregulates the HR, its transcription factor activity not being essential for this inhibition. P53 is the most commonly mutated tumor suppressor protein. Some p53 mutants (e.g. 273L) have lost the ability to downregulate the HR, but not all of them: Cells containing the p53 mutant M237I showed an increased recombination activity and increased spontaneous and x-ray induced mutation frequencies in comparison to wt p53 cells.

We reproduced the suppression of HR by the dominant-negative p53 mutant 273L in A549 cells and concluded the transcription factor activity not being essential for the suppression of the HR activity. The p53M237I mutant expressing cells showed higher HR activity levels than wt p53 and p53QS expressing cells. The increased HR activity was seen in p53M237I pooled population cells as well as in single clone derived cells: Results are compatible with p53 mutant M237I being a gain-of-function mutant.

In p53M237I cells we additionally saw more DSBs marked by 53BP1 than in wt p53 and p53QS cells and concluded the HR activity could be due to more DNA DSBs. All three H1299 cell lines (H1299FRT/p53QS, H1299FRTzeo and H1299FRT/p53M237I) showed RPA foci after the treatment with thymidine (5mM, 24h).

We propose the protein p53 taking part in the replication fork stabilization similar to the protein ATR. There is evidence that p53 is part of the ATR-checkpoint.

SUPPLEMENT
7 LISTINGS OF ALL MATERIALS

Cell line	Cell line specifications
H1299	- NSCLC cell line - Cultivation in RPMI 1640 medium - Purchased by ATCC (American Type Culture Collection)
H1299FRT/p53QS H1299FRT/p53QM H1299FRTzeo	- Constructed by Willers et al. (unpublished)
H1299FRT/p53M237I	- Constructed by Wülfing (unpublished)
A549	- NSCLC cell line - Cultivation in DMEM medium - Purchased by ATCC
A549cDNA A549/p53-273L	- Constructed by Willers et al. (unpublished)
Mycoplasma Detection Kit	- MycoAlert® Mycoplasma Detection Kit (Lonza LT07-318)

Media for cell culture

Media base	Additives added for cell culture
RPMI 1640 DMEM	- SIGMA - SIGMA All media supplemented with addition of: - 10% BGS (HyClone) - 2% HEPES (SIGMA,H4034) - 1% L-Glutamine (CELLGRO, 25-005-C1)

	- 1% Penicillin-Streptomycin (CELLGRO)
Hygromycin B	- selection antibiotic for maintenance of H1299FRT/p53QS and H1299FRT/p53QM - 200µg/ml in the medium - invitrogen 10687010

Further materials used for keeping cells in culture

Material	**Material specifications**
1x PBS	
1x Trypsin	- SIGMA, H4034
T25 culture flask	- 25cm^2 flask (BD Falcon 353109)
T75 culture flask	- 75cm^2 flask (BD Falcon 353136)
Incubator	- Humidified, 37°C, 5% CO^2 (Forma Scientific)
Hood	- Steril Guard Hood (Baker Company, Inc.) and Class II Type A/B3 (Nuaire Biological Safety Cabinets)
Microscope	- Nikon Eclipse TS100
Counting Grid	- Reichert Bright-Line Hematocytometer
Sterilizer	- Harvey SterileMax™
15ml/50ml Tubes	- BlueMax (BD Falcon 352097 and 352098)
Water bath	- National Appliance Company Model 220
Pipetts	- 1ml/2ml Serological Pipet (Falcon 357520 and 357507)

	- 5ml/10ml (Fisherbrand Pipets 13-678-27E and 13-678-27E) - 25ml/50ml Costar. Stripette (Corning Incorporated 4489 and 4490)
Gloves	- Purple Nitrile (Kimberly-Clark)

Materials used for freezing cells

Material	**Material specifications**
Dimethyl Sulfoxide (DMSO)	- SIGMA D4540
Centrifuge	- Thermo Electron Corporation IEC and Beckman Coulter Allegra 6
-20℃ freezer	- General Electric
-70℃ freezer	- VWR Scientific
Liquid Nitrogen Tank	- Cyromed (Forma Scientific Inc.)
Vials for freezing	- Cyrogenic vials (Nunc 377267)

Materials for Immunofluorescence microscopy

Material	**Specifications**
Culture Slides	- 8 chamber polystyrene vessel, BD Falcon 354108
Thymidine	- SIGMA T1895
Hydroxyurea	- SIGMA H8627
Balance	- Denver Instrument Company TL-104
<u>Permeabilization Buffer:</u>	
0.5% Triton X	- SIGMA T9284
20mM HEPES	- pH 7.9, Siena
50mM NaCl	- SIGMA, S5886
3mM KCl	- SIGMA, P4504

300mM Sucrose Fixation Buffer: 3% PFA 2% Sucrose 1x PBS Blocking Buffer: 0.5% NP40 10% Bovine Growth Serum (BGS) 0.3% NaN_3 1x PBS Milk powder Goat serum DAPI Antifade Translucent Nail polish BSA Cover glass	- SIGMA, S7903 - Boston Bioproducts, BM-155 - SIGMA, S7903 - Calbiochem, 492015 - Hyclone, SH30541.03 - SIGMA, S-8032 - Blotting grade Non Fat Dry Milk (BioRad) - SIGMA 28718-90-3 - Vectashield Mounting Medium for Fluorescence (Vector Laboratories Inc., H-1000) - N.Y.C - SIGMA - Premium Cover Glass (Fisher Scientific 12-548-5E)
Primary antibodies	
Rad51	Anti Rad51 Rabbit pAb (Calbiochem PC130)
gamma-H2AX	Mouse mAb to gamma-H2AX (abcam ab18311-100)
53BP1	Rabbit pAb to 53BP1 (abcam ab21083-100)
RPA	RPA/p34 Ab-1 (9H8) Mouse MAb (Neo Markers Fremont CA MS-691-PO)

Secondary antibodies	
2nd Antibody to Rad51 and 53BP1	Alexa Fluor 488 chicken anti-rabbit (invitrogen A21441)
2nd Antibody to gamma-H2AX and RPA	Alexa Fluor 488 goat anti-mouse (invitrogen A11004)

Materials for amplifying plasmid DNA

Materials	Specifications
Electroporation Cuvette	- 1mm Gap (Fisher Biontech, FB101)
Electroporator	- BioRad Micropulser
Electrocompetent cells	- ElectroMax DH10B Cells (invitrogen, 18290-015)
S.O.C. Medium	- invitrogen 15544-034
14ml Tube	- Round-Bottom Polypropylene Tube (BD Falcon 352059)
Ampicillin tablets	- Ampicillin Tablets, 2.5mg/Tablet and 25mg/Tablet (Stratagene 300020-61 and 300021-61)
Disposable Inoculating Loop	- Fisherbrand 22-363-604
37℃ bacterial shaker	- Lab-Line-Instruments Inc.
37℃ bacterial incubator	- Precision incubator
Spectrophotometer	- Perkin Elmer

Materials for purification of plasmid DNA

Materials	Specifications
Plasmid purification Kit	- QIAGEN® Plasmid Maxi Kit (Qiagen 12162)
Centrifuge	- Microfuge 18 Centrifuge (Beckman Coulter) - Sorvall RC 5C Plus

	(Kendro Laboratory Products)
Rotor for Centrifuge	- Sorvall SLA-600TC and SLA-500 (Kendro Laboratory Products)
200ml-Tube for Sorvall Centrifuge	
50ml Tube	- BlueMax (BD Falcon 352098)
Sterile 1.5ml tubes	- Sterile 1.5ml eppendorf tubes
Ethanol	- 200 proof (absolute) (Sigma-Aldrich E7023)
Isopropanol	- Sigma-Aldrich I9516
pH meter	- Corning Incorporated 430

Materials for DNA quantification

Materials	**Specifications**
ddH_2O	- Milli-Q Reagent Water System 650-C
Spectrophotometer	- GeneQuant pro (Amersham Biosciences)
Glass micro cells for spectrophotometers	- 500µl (Fisher scientific 14-385-928A)

DNA restriction digest of pcDNAp53M237I#1 and pcDNAp53M237I#2

Materials	**Specifications**
Microwave	- Panasonic, Inverter
Agarose	- BioRad 162-0102
Ethidium Bromide	- 10mg/ml, Sigma E1510
Loading dye	- Orange G loading dye (6x) (Boston BioProducts BM-102G)
DNA ladder	- Quick-Load 1kb DNA ladder (New England Biolabs N0468S)
Purified BSA (100x)	- 10mg/ml (New England Biolabs B9001S)

NE Buffer 3 (10x)	- New England Biolabs B7003S
Restriction Enzyme PvuI	- 10,000U/ml (New England Biolabs R0150S)
UV light imaging	- Gene Flash by Syngene Bio Imaging
Printer	- Sony Corporation UP-895MD

Materials for stable integration of pcDNAp53Ile237

Materials	**Specifications**
Serum-antibiotic-free-medium	- Regular medium but only added 2% HEPES and 1% L-Glutamine
Transfection reagent	- Metafectene pro (Biontex T040)
Tissue culture dish	- 100 x 15mm (Fisherbrand 08-757-12)

Materials for total cell lysates

Materials	**Specifications**
Tissue culture dish	- 100 x 15mm (Fisherbrand 08-757-12)
1x PBS	- cooled on ice
Cell Extraction Buffer	- Biosource Buffer (invitrogen FNN0011)
Protease Inhibitor Cocktail phenylmethylsulfonyl fluoride (PMSF)	- Fluka, 78830
Cell Scraper	- Disposable Cell Scraper (Fisherbrand 08-773-2)
1.5ml tubes	- eppendorf
Centrifuge	- Microfuge® 18 Centrifuge (Beckman Coulter 367160)

Materials for protein concentration assay

Materials	Specifications
Photometer	- GeneQuant Pro (Amersham Biosciences 80-2115-04)
Calibration Solution	- 1mg/ml BSA stock solution, Albumine Bovine Serum (SIGMA)
Protein Dye	- Protein Assay Dye Reagent Concentrate (BioRad 500-0006EDU)
ddH_2O	- Milli-Q Reagent Water System 650-C

Materials for running western blot gel

Materials	Specifications
Heatblock	- Select Heatblock (VWR Scientific Products 1774)
Gel	- NuPAGE® Novex® 4-12% Bis-Tris Mini Gel 1mm x 10 wells (invitrogen NP0321)
Electrophoresis Box	- XCell Surelock Mini Cell (invitrogen EI0001)
Sample Buffer	- LDS Sample Buffer (4x) (invitrogen NP0007)
Sample reducing agent	- Sample reducing agent (10x) (invitrogen NP0009)
Molecular Weight ladder	- Novex® Sharp Pre-stained Protein Standard (invitrogen LC5800)
MES SDS Running Buffer	- NuPAGE® MES SDS Running Buffer (20x) (invitrogen NP00002)
Power supply	- Power Pac 200 (BioRad 284BR 16609)

Materials for transferring western blot gel

Materials	Specifications
Transfer Cell	- Mini Trans-Blot Cell (BioRad 170-3930)
Transfer Sandwich	- Mini Protean 3 cell sandwich (BioRad 165-3301)
Filter paper for sandwich	- PVDF membrane, 0.2µm pore size (invitrogen LC2002)
Transfer Buffer	- NuPAGE® Transfer Buffer (20x) (invitrogen NP0006-1)
Power supply	- Power Pac HC (BioRad 043BR 13301)
Blotting Membrane	- Whatman Pure Cellulose Blotting Sheets, 3MM Chromography (Whatman 3030-917)
Blocking buffer	- 5% dried milk, Blotting grade Non Fat Dry Milk (BioRad) - 0.1% T-TBS
Knife	- Gel Knife (invitrogen)
Shaker	- HybriShaker (Thomas Scientific 7746-S0005)

Materials for blotting for p53 and filamin

Primary antibodies	Specifications
Anti-p53	- Anti-p53 (Ab-7) (Pantropic) Sheep pAb (Calbiochem PC35)
Filamin	- Filamin 1 (E-3) mouse monoclonal IgG_2a (Santa Cruz Biotechnology sc-17749)
Secondary antibodies	**Specifications**
2^{nd} Antibody for p53	- goat anti-mouse IgG-HRP (Santa

	Cruz Biotechnology sc-2031)
2nd Antibody for Filamin	- donkey anti-sheep IgG-HRG (Santa Cruz Biotechnology sc-2473)
Materials	**Specifications**
Blocking buffer	- 5% dried milk, Blotting grade Non Fat Dry Milk (BioRad) - 0.1% T-TBS

Materials for membrane exposure

Materials	**Specifications**
Transparencies	
ECl reagents	- Pierce SuperSignal West Pico ECL reagents 32109
Film Cassette	- Radiation Therapy Cassette 25x30cm (Dupont Cronex)
Film	- Kodak BioMax Light Film 13x18cm
Film developing machine	
Scanner	- Epson Perfection 2480 Photo
Image Software	- Adobe Photoshop 7.0

Materials for analysis of relative expression levels of proteins

Materials	**Specifications**
Scanner	- Epson Perfection 2480 Photo
Imaging Software	- Adobe Photoshop 7.0 - ImageJ
Spreadsheet application software	- Microsoft Office Excel 2007
Plotting software	- GraphPad Prism 5

8 ABBREVIATIONS

A549	Non-small cell lung cancer cell line
ATM	Ataxia telangiectasia mutated protein
ATP	Adenosine triphosphate Ataxia
ATR	Telangiectasia and Rad3-related protein
BGS	Bovine growth serum
BLM	Bloom syndrome gene
BRCA1	Breast cancer type 1 susceptibility protein
BRCA2	Breast cancer type 2 susceptibility protein
℃	degree celsius
CO_2	Carbon dioxide
DAPI	4',6-diamidino-2-phenylindole
ddH_2O	double-distilled water
DANN	Deoxyribonucleic acid
DSB	DNA double-strand break
DSBs	DNA double-strand breaks
ECL	Electrochemiluminescence
E.coli	Escherichia coli
EDTA	Ethylenediaminetetraacetic acid
e.g	for example
et al.	et alii which means “and others”
Fig.	Figure
FRT	Flp recombinase target

G418	Geneticin; selection antibiotics
Gamma-H2AX	DNA double-strand break marker
H	Hour
H1299	Non-small cell lung cancer cell line
H2AX	Histone H2A
HEPES	4-(2-hydroxyethyl)-1-piperazineethanesulfonic acid
HPRT	Hypoxanthine-guanine phosphoribosyltransferase
HR	homologous recombination
Hrs	Hours
Kb	Kilobases
KCl	Potassium chloride
kDa	Kilo Dalton
Mdm2	Murine double minute oncogene
MES	2-(N-morpholino)ethanesulfonic acid
Min	minute; minutes
mM	Millimolar
MRN	Mre11-Rad50-Nbs1 heterotrimeric protein complex
NaCl	Sodium chloride
NaN_3	Sodium azide
NHEJ	Non-homologous end-joining
Nm	Nanometer
NP40	Nonyl phenoxypolyethoxylethanol
NSCLC	Non-small cell lung cancer

OD	Optical density
OD600	Optical density at wavelength 600nm
PBS	Phosphate buffered saline
PFA	Paraformaldehyde
PMSF	Phenylmethanesulfonylfluoride
Rad51	Key protein in the homologous recombination
RAD52	Protein involved in DNA double-strand break repair and HR
RAD54	Protein in homologous recombination
RPA	Replication Protein A
SDS	Sodium dodecyl sulfate
S.O.C.	Derivate of super optimal broth medium
ssDNA	Single-stranded DANN
TAE	Buffer solution containing tris base, acetic acid and EDTA
TE	Buffer containing Tris, EDTA and Mg^{2+}
TK	Thymidine kinase
P53	Tumor suppressor gene p53
TrisCl	tris(hydroxymethyl)amino methane
UV	Ultraviolet light
V	Volt
WRN	gene; mutations in this gene cause Werner Syndrome
Wt	Wildtype
WHO	World Health Organization
x-ray	x-radiation

9 TABLE OF FIGURES

10 REFERENCES

1. Akyüz N, Boehden GS, Süsse S, et al. DNA substrate dependence of p53-mediated regulation of double-strand break repair. *Mol Cell Biol*. 2002;22(17):6306-6317.

2. Albrechtsen N, Dornreiter I, Grosse F, et al. Maintenance of genomic integrity by p53 complementary roles for activated and non-activated p53. *Oncogene*. 1999;18(53):7706-7717.

3. Banáth JP, Olive PL. Expression of Phosphorylated Histone H2AX as a Surrogate of Cell Killing by Drugs that Create DNA Double-Strand Breaks. *Cancer Res*. 2003;63:4347-4350.

4. Bishop AJR, Hollander MC, Kosaras B, et al. Atm-, p53-, and Gadd45a-Deficient Mice show an Increased Frequency of Homologous Recombination at Different Stages during Development. *Cancer Res*. 2003;63:5335-5343

5. Bode AM, Dong Z. Post-translational modification of p53 in tumorigenesis. *Nat Rev Cancer*. 2004;4:793-805.

6. Boehden GS, Akyüz N, Roemer K, Wiesmüller L. p53 mutated in the transactivation domain retains regulatory functions in homology-directed double-strand break repair. *Oncogene*. 2003;22:4111-4117.

7. Bonner WM, Redon CE, Dickey JS, et al. gamma-H2AX and cancer. *Nat Rev Cancer*. 2008;8:957-967.

8. Bossi G, Lapi E, Strano S, et al. Mutant p53 gain of function: reduction of tumor malignancy of human cancer cell lines through abrogation of mutant p53 expression. *Oncogene*. 2006;25(2):304-309.

9. Bossi G, Marampon F, Maor-Aloni R, et al. Conditional RNA interference in vivo to study mutant p53 oncogenic gain of function on tumor malignancy. *Cell Cycle*. 2008;7(12):1870-1879.

10. Boulon S, Westman BJ, Hutten S, Boisvert F-M, Lamond AI. The Nucleolus under Stress. *Mol Cell*. 2010;40(2):216-227.

11. Branzei D, Foiani M. Regulation of DNA repair throughout the cell cycle. *Nat Rev Mol Cell Biol*. 2008;9:297-308.

12. Breuer RHJ, Postmus PE, Smit EF. Molecular pathology of NSCLC. *Respiration*. 2005;72:313-330.

13. Brosh R, Rotter V. When mutants gain new powers: news from the mutant p53 field. *Nat Rev Cancer*. 2009;9:701-713.

14. Buchhop S, Gibson MK, Wang XW, et al. Interaction of p53 with the human Rad51 protein. *Nucleic Acids Res*. 1997;25(19):3868-3874.

15. Chuang Y-YE, Chen Q, Liber HL. Radiation-induced Mutations at the Autosomal Thymidine Kinase Locus Are Not Elevated in p53-null Cells. *Cancer Res*. 1999;59:3073-3076.

16. Cimprich KA, Cortez D. ATR: an essential regulator of genome integrity. *Nat Rev Mol Cell Biol*. 2008;9:616-627.

17. Cohn MA, D'Andrea AD. Chromatin Recruitment of DNA Repair Proteins: LEssons from the Fanconi Anemia and Double-Strand Break Repair Pathways. *Mol Cell*. 2008;32:306-312.

18. Fernandez-Capetillo O, Chen H-T, Celeste A, et al. DNA damage-induced G2-M checkpoint activation by histone H2AX and 53BPI. *Nat Cell Biol*. 2002;Vol. 4:993-997.

19. FitzGerald JE, Grenon M, Lowndes NF. 53BP1: function and mechanisms of focal recruitment. *Biochem Soc Trans*. 2009;37(4):897-904.

20. Fragkos M, Jurvansuu J, Beard P. H2AX is required for cell cycle arrest via the p53/p21 pathway. *Mol Cell Biol*. 2009;29(10):2828-2840.

21. Gatz SA, Wiesmüller L. p53 in recombination and repair. *Cell Death Differ*. 2006;13:1003-1016.

22. Golub EI, Gupta RC, Haaf T, Wold MS, Radding CM. Interaction of human rad51 recombination protein with single-stranded DNA binding protein, RPA. *Nucleic Acids Res*. 1998;26(23):5388-5393.

23. Hainaut P, Hollstein M. p53 and human cancer: the first ten thousand mutations. *Adv Cancer Res*. 2000;77:81-137.

24. Hartlerode AJ, Scully R. Mechanisms of double-strand break repair in somatic mammalian cells. *Biochem J*. 2009;423:157-168.

25. Helleday T, Lo J, van Gent DC, Engelward BP. DNA double-strand break repair: from mechanistic understanding to cancer treatment. *DNA repair (Amst)*. 2007;6(7):923-935.

26. Iftode C, Daniely Y, Borowiec JA. Replication protein A (RPA): the eukaryotic SSB. *Crit Rev Biochem Mol Biol*. 1999;34(3):141-180.

27. Ismail IH, Hendzel MJ. The gamma-H2A.X: Is It Just a Surrogate Marker of Double-Strand Breaks or Much More? *Environ Mol Mutagen*. 2008;49:73-82.

28. Jackson SP, Bartek J. The DNA-damage response in human biology and disease. *Nature*. 2009;461:1071-1078.

29. Janz C, Wiesmüller L. Wild-type p53 inhibits replication-associated homologous recombination. *Oncogene*. 2002;21:5929-5933.

30. Kaneuchi M, Yamashita T, Shindoh M, et al. Induction of apoptosis by the p53-273L (Arg --> Leu) mutant in HSC3 cells without transactivation of p21Waf1/Cip1/Sid1 and bax. *Mol Carcinog*. 1999;26(1):44-52.

31. Kantake N, Sugiyama T, Kolodner RD, Kowalczykowski SC. The Recombination-deficient Mutant RPA (rfa1-t11) Is Displaced Slowly from Single-stranded DNA by Rad51 Protein. *J Biol Chem*. 2003;278(26):23410-23417.

32. Keimling M, Wiesmüller L. DNA double-strand break repair activities in mammary epithelial cells--influence of endogenous p53 variants. *Carcinogenesis*. 2009;30(7):1260-1268.

34. Kinner A, Wu W, Staudt C, Iliakis G. gamma-H2AX in recognition and signaling of DNA double-strand breaks in the context of chromatin. *Nucleic Acids Res*. 2008;36(17):5678-5694.

35. Kobayashi J, Iwabuchi K, Miyagawa K, et al. Current topics in DNA double-strand break repair. *J Radiat Res (Tokyo)*. 2008;49(2):93-103.

36. Levine AJ, Oren M. The first 30 years of p53: growing ever more complex. *Nat Rev Cancer*. 2009;9:749-758.

37. Li X, Heyer W-D. Homologous recombination in DNA repair and DNA damage tolerance. *Cell Res*. 2008;18:99-113.

38. Lundin C, Erixon K, Arnaudeau C, et al. Different Roles for Nonhomologous End joining and Homologous Recombination following Replication arrest in mammalian cells. *Mol Cell Biol*. 2002;22(16):5869-5878.

39. Ma X, Vataire AL, Sun H, et al. TP53 and KRAS Mutations as Markers of Outcome of Adjuvant Cisplatin-Based Chemotherapy in Completely Resected Non-Small-Cell Lung Cancer (NSCLC): The International Adjuvant Lung Cancer Trial (IALT) BBiological Program. *Ann Oncol Abstr*. 2008;19:viii61-62.

40. Marková E, Schultz N, Belyaev IY. Kinetics and dose-response of residual 53BPI/-H2AX foci: Co-localization, relationship with DSB repair and clonogenic survival. *Int J Radiat Biol*. 2007;83(5):319-329.

41. Meek DW. Tumour suppression by p53: a role for the DNA damage response? *Nat Rev Cancer*. 2009;9(10):714-723.

42. Olivier M, Petitjean A, Marcel V, et al. Recent advances in p53 research: an interdisciplinary perspective. *Cancer Gene Ther*. 2009;16:1-12.

43. Paulsen RD, Cimprich KA. The ATR pathway: Fine-tuning the fork. *DNA repair (Amst)*. 2007;6:953-966.

44. Petermann E, Helleday T. Pathways of mammalian replication fork restart. *Nat Rev Mol Cell Biol*. 2010;11:683-687.

45. Petermann E, Orta ML, Issaeva N, Schultz N, Helleday T. Hydroxyurea-Stalled Replication Forks Become Progressively Inactivated and Require Two Different RAD51-Mediated Pathways for Restart and Repair. *Mol Cell*. 2010;37:492-502.

46. Postow L, Crisona NJ, Peter BJ, Hardy CD, Cozzarelli NR. Topological challenges to DNA replication: Conformations at the fork. *Proceedings Of The National Academy Of Sciences Of The United States Of America*. 2001;98(15):8219-8226.

47. Reliene R, Bishop AJR, Schiestl RH. Involvement of homologous recombination in carcinogenesis. *Adv Genet*. 2007;58:68-87.

48. Restle A, Färber M-, Baumann C, et al. Dissecting the role of p53 phosphorylation in homologous recombination provides new clues for gain-of-function mutants. *Nucleic Acids Res*. 2008;36(16):5362-5375.

49. Robison JG, Dixon K, Bissler JJ. Cell cycle-and proteasome-dependent formation of etoposide-induced replication protein A (RPA) or Mre11/Rad50/Nbs1 (MRN) complex repair foci. *Cell Cycle*. 2007;6(19):2399-2407.

50. Rogakou EP, Pilch DR, Orr AH, Ivanova VS, Bonner WM. DNA double-stranded breaks induce histone H2AX phosphorylation on serin 139. *J Biol Chem*. 1998;273:5858-5868.

51. Romanova LY, Willers H, Blagosklonny MV, Powell SN. The interaction of p53 with replication protein A mediates suppression of homologous recombination. *Oncogene*. 2004;23:9025-9033.

52. Rothkamm K, Horn S. gamma-H2AX as protein biomarker for radiation exposure. *Ann Ist Super Sanita*. 2009;45(3):265-271.

53. Saintigny Y, Delacote F, Varès G, et al. Characterization of homologous recombination induced by replication inhibition in mammalian cells. *EMBO J*. 2001;20(14):3861-70.

54. Schild D, Wiese C. Overexpression of Rad51 suppresses recombination defects: a possible mechanism to reverse genomic instability. *Nucleic Acids Res*. 2009;(doi:10.1093/nar/gkp1063):1-10.

55. Sedelnikova OA, Bonner WM. gamma-H2AX in Cancer Cells. *Cell Cycle*. 2006;5(24):2909-2913.

56. Sengupta S, Harris CC. p53: traffic cop at the crossroads of DNA repair and recombination. *Nat Rev Mol Cell Biol*. 2005;6:44-55.

57. Shaulsky G, Goldfinger N, Rotter V. Alterations in Tumor Development in Vivo Mediated by Expression of Wild Type or Mtant p53 Proteins. *Cancer Research*. 1991;51:5232-5237.

58. Sirbu BM, Lachmayer SJ, Wülfing V, et al. ATR-p53 Restricts Homologous Recombination in Response to Replicative Stress but Does Not Limit DNA Interstrand Crosslink Repair in Lung Cancer Cells. *PLoS ONE*. 2011;6(8):e23053.

59. Sonoda E, Zhao GY, Kohzaki M, et al. Collaborative roles of gamma-H2AX and the Rad51 paralog Xrcc3 in homologous recombinational repair. *DNA repair (Amst)*. 2007;6:280-292.

60. Srivastava N, Gochhait S, de Boer P, Bamezai RNK. Role of H2AX in DNA damage response and human cancers. *Mutat Res*. 2009;681(2-3):180-188.

61. Trenz K, Smith E, Smith S, Constanzo V. ATM and ATR promote Mre11 dependent restart of collapsed replication forks and prevent accumulation of DNA breaks. *EMBO J*. 2006;25:1764-1774.

62. Wang X, Haber JE. Role of Saccharomyces Single-Stranded DNA-Binding Protein RPA in the Strand Invasion Step of Double-Strand Break Repair. *PLoS Biol*. 2004;2(1):0104-0112.

63. Willers H, McCarthy EE, Wu B, et al. Dissociation of p53-mediated suppression of homologous recombination from G1/S cell cycle checkpoint control. *Oncogene*. 2000;19(5):632-639.

64. Xia F, Amundson SA, Nickoloff JA, Liber HL. Different Capacities for Recombination in Closely Related Human Lymphoblastoid Cell Lines with Different Mutational Responses to X-irradiation. *Mol Cell Biol*. 1994;14(9):5850-5857.

65. Xia F, Liber HL. The tumor suppressor p53 modifies mutational processes in a human lymphoblastoid cell line. *Mutat Res*. 1997;373(1):87-97.

66. Xia F, Wang X, Wang YH, et al. Altered p53 status correlates with differences in sensitivity to radiation-induced mutation and apoptosis in two closely related human lymphoblast lines. *Cancer Res*. 1995;55(1):12-15.

67. Xu Y. Induction of genetic instability by gain-of-function p53 cancer mutants. *Oncogene*. 2008;27:3501-3507.

11 ACKNOWLEDGEMENTS

I would like to thank Prof. Dr. med. Jochen Dahm-Daphi and Dr. med. Henning Willers for choosing me in this project and giving me the opportunity to do the experimental work in cooperation with the laboratory in Hamburg and Boston. Prof. Dr. med. Dahm-Daphi and Dr. med. Willers both showed a lot of patience and good advice and always had time for questions and problem solving during the experimental and writing progress. I have learned a lot of important things about science and research in this time. I very much appreciate their support and help.

Liliana Gheorghiu introduced me to the lab work and supervised the experimental work. Thank you very much for the support and the great work atmosphere.

Priyanjali Ghosh has taken care of my cells from time to time. She also has given me good advice for foci staining. Thank you.

Fruzsina Gatzemeier introduced me to cell culture and steril work. I want to thank her for her technical help and support.

I would like to thank Chake Tokadjian for her technical help.

Special thanks goes to my loved parents and sisters. Without you I would not have been able to do this. All my life you have believed in me and supported me no matter what I wanted to do. Thank you.

I would like to thank Adam Dybulla. You supported me in every possible way no matter what time or day. I am grateful for knowing such a wonderful person you are.

Last but not least a big thank you to my friends for their emotional support and great friendship.

12 CURRICULUM VITAE

entfällt aus datenschutzrechtlichen Gründen

13 STATEMENT OF ORIGINALITY

I herewith declare that I have performed the work for this thesis independently and without improper help. This work does not contain any material written or published by another person except where acknowledged. References in word or content are stated with edition, year, volume and page. I have listed all persons who directly participated in the process of this thesis. This body of work has not previously been submitted for a degree at this or any other university.

20th June 2012 Verena Wülfing